Fig. 4. Leishmania major-parasitized Rag-2$^{-/-}$ splenocytes mixed with parasitized B10.D2 CD11c$^+$ DCs lead BALB/c WT mice to mild outcome of the disease and T_h1 response. (A–C) DC-depleted L. major-parasitized BALB/c-Rag-2$^{-/-}$ splenocytes were mixed with parasitized CD11c$^+$ DCs from BALB/c (open circles and open bars) or B10.D2 (closed circles and closed bars). (D–F) DC-depleted L. major-parasitized B10.D2-Rag-2$^{-/-}$ splenocytes were mixed with parasitized CD11c$^+$ DCs from BALB/c (open squares and open bars) or B10.D2 (closed squares and closed bars). Parasitized cells (10^7 per mouse) were inoculated into BALB/c mice. (A and D) Footpad swelling caused by L. major infection. (B and E) Parasite burdens in footpads and popliteal lymph nodes of infected legs. +, mean of each group. (C and F) IFN-γ and IL-4 production from splenocyte stimulation with parasite antigens. Statistical significance: *P < 0.01, **P < 0.001 and ***P < 0.0001

parasites determine the outcome of infection including footpad swelling, parasite burden and immune responses upon L. major infection. Those cells likely include macrophages and DCs.

Genetic background of CD11c$^+$ DCs determines outcome of disease

L. major promastigotes are able to penetrate into DCs in addition to macrophages (16–18). Since DCs are known to be the only antigen-presenting cells (APCs) capable of activating naive T cells (19), they are likely candidates determining the immune response upon L. major infection. To this end, CD11c$^+$ DCs were removed from L. major-parasitized Rag-2$^{-/-}$ splenocytes using anti-CD11c coupled magnetic beads before inoculating into WT mice. As shown in Fig. 3(D–F), the outcome of disease by inoculation with DC-depleted parasitized B10.D2-Rag-2$^{-/-}$ splenocytes was dramatically changed as compared with untreated parasitized cells (Fig. 3D and E, closed circles). As revealed by progressive footpad swelling and high parasite burdens in the footpad as well as in the popliteal lymph node, BALB/c WT mice inoculated with DC-depleted parasitized B10.D2-Rag-2$^{-/-}$ splenocytes exhibited nearly the same degree of severity as the mice inoculated with DC-depleted parasitized BALB/c-Rag-2$^{-/-}$ splenocytes (Fig. 3D and E, open circles). Notably, both groups of mice were unable to mount T_h1 immune responses (Fig. 3F, open and gray bars). We observed little effect of DC depletion when parasitized splenocytes were inoculated into syngeneic WT mice (e.g. open circles in Fig. 3A and D and open squares in Fig. 3A and D). It is likely that DCs of recipient mice captured L. major and elicited immune responses.

To further examine the importance of DCs, DC-depleted parasitized Rag-2$^{-/-}$ splenocytes were reconstituted with parasitized DCs and inoculated into BALB/c WT mice. As shown in Fig. 4, when mice were inoculated with DC-depleted parasitized BALB/c-Rag-2$^{-/-}$ splenocytes together with parasitized B10.D2-DCs, those mice exhibited milder symptoms and induced a T_h1-dominant response (Fig. 4A–C, closed symbols). Such milder symptoms were not observed with parasitized BALB/c-DCs. Moreover, when mice were inoculated with DC-depleted parasitized B10.D2-Rag-2$^{-/-}$ splenocytes together with parasitized BALB/c-DCs, they exhibited the exacerbated symptoms and resulted in a T_h2-dominant response (Fig. 4D–F, open symbols). Collectively, these results indicate that DCs are indeed the cells that carry genetic factors determining the susceptibility to L. major infection. Essentially, the same results were obtained using BMDCs instead of splenic CD11c$^+$ DCs (data not shown).

Discussion

Our present results collectively indicate that DCs carry genetic factors determining the T_h1/T_h2 balance and outcome of L. major infection. It is intriguing that macrophages are not involved in determining the T_h1/T_h2 balance. Although macrophages are able to present antigens, macrophages present microbial antigens to differentiated effector cells, especially T_h, to receive cytokines from T_h at the site of infection. On the other hand, DCs activate naive T cells into effector cells in secondary lymphoid organs. Such differences may contribute to the critical role of DCs in determining the T_h1/T_h2 balance.

A previous report has implicated that the genetic difference in susceptibility to L. major is determined by both T and

non-T cells by similar experiments using athymic BALB/c recipients reconstituted with T cells from C57BL/6.C-H-2^d congenic mice (20). However, all BALB/c-Rag-$2^{-/-}$ mice reconstituted with B10.D2 T cells exhibited a body weight loss and hair loss and half of these mice died within 3 months (K. Suzue and S. Koyasu, unpublished observation) likely due to the chronic graft versus host reaction by mis-matching minor histocompatibility antigens such as minor lymphocyte-stimulating superantigen (21). We were therefore unable to compare the difference between B10.D2-Rag-$2^{-/-}$ mice with BALB/c CD4$^+$ T cells and BALB/c-Rag-$2^{-/-}$ mice with B10.D2 CD4$^+$ T cells.

At the moment, little is known about factors specifically expressed in DCs. Among cytokines produced by DCs, IL-12 is a pivotal cytokine inducing the T_h1 response and is one of likely candidates. However, involvement of IL-12 in the difference between *L. major*-susceptible and -resistant strains is unclear. Previous studies have shown that there is no difference between fetal skin-derived DCs from C57BL/6 and BALB/c in their ability to produce IL-12 in response to *L. major* amastigotes (18, 22). Other studies have also observed little difference in the production of IL-12 by DCs from C57BL/6 and BALB/c mice in response to various stimuli (23). *L. major* infection *in vitro* induced IL-12 release from splenic DCs and splenic DCs from B10.D2 mice produced slightly higher amounts of IL-12 than those from BALB/c mice in our hands (K. Suzue and S. Koyasu, unpublished observation). However, it is unclear if the amount of IL-12 produced by DCs is the only factor determining T_h1/T_h2 balance in *L. major* infection.

It is generally accepted that the T_h1/T_h2 balance in *L. major* infection is a polygenic phenomenon (24). Indeed, in addition to IL-12 handful factors have been reported that affect T_h1/T_h2 balance in a strain-dependent manner. Trans-forming growth factor-β is known to block T_h1 differentiation at lower doses in BALB/c mice than in other strains of mice by controlling IL-12 receptor expression on T cells (25). IL-1 and tumor necrosis factor-α have been reported as critical factors in BALB/c but not in C57BL/6 mice for the induction of T_h1 response (26, 27). Chemokine/chemokine receptor system is also an important factor that determines the outcome of *L. major* infection (28). These cytokines/chemokines are produced by DCs but by other cell types as well. There was no significant difference in the amounts of IL-1 produced by DCs between B10.D2 and BALB/c mice (K. Suzue and S. Koyasu, unpublished observation). Furthermore, there was no difference in the up-regulation of cell-surface markers including B7 and MHC class II molecules on splenic DCs between these two strains (K. Suzue and S. Koyasu, unpublished observation).

Tpm1 locus is known to control IL-12 responsiveness in a cell-autonomous manner (29). However, *Tmp1* controls IL-12 responsiveness of T cells and our results exclude the involvement of T cells. It was shown that the early administration of IL-4 stimulates DCs to produce IL-12 and protect BALB/c mice from *L. major* infection (30). Such responsiveness of DCs to IL-4 may be important in determining the susceptibility to *L. major* infection. Finally, prostaglandin E_2 (PGE$_2$) suppresses IL-12p70 production and BALB/c APCs express higher levels of PGE$_2$ receptors than those of other strains, making BALB/c APCs more sensitive to PGE$_2$ (31). These possibilities should be examined in future studies.

Abbreviations

APC	antigen-presenting cell
BM	bone marrow
BMDC	bone marrow-derived dendritic cell
DC	dendritic cell
PGE$_2$	prostaglandin E_2
WT	wild type

References

1 Mosmann, T. R. and Sad, S. 1996. The expanding universe of T-cell subsets: Th1, Th2 and more. *Immunol. Today* 17:138.
2 Reiner, S. L. and Locksley, R. M. 1995. The regulation of immunity to *Leishmania major*. *Annu. Rev. Immunol.* 13:151.
3 Scott, P., Natovitz, P., Coffman, R. L. *et al.* 1988. Immunoregulation of cutaneous leishmaniasis. T cell lines that transfer protective immunity or exacerbation belong to different T helper subsets and respond to distinct parasite antigens. *J. Exp. Med.* 168:1675.
4 Holaday, B. J., Sadick, M. D., Wang, Z. E. *et al.* 1991. Reconstitution of *Leishmania* immunity in severe combined immunodeficient mice using Th1- and Th2-like cell lines. *J. Immunol.* 147:1653.
5 Mougneau, E., Altare, F., Wakil, A. E. *et al.* 1995. Expression cloning of a protective *Leishmania* antigen. *Science* 268:563.
6 Launois, P., Maillard, I., Pingel, S. *et al.* 1997. IL-4 rapidly produced by Vβ4 Vα8 CD4$^+$ T cells instructs Th2 development and susceptibility to *Leishmania major* in BALB/c mice. *Immunity* 6:541.
7 Sadick, M. D., Heinzel, F. P., Holaday, B. J. *et al.* 1990. Cure of murine leishmaniasis with anti-interleukin 4 monoclonal antibody. Evidence for a T cell-dependent, interferon γ-independent mechanism. *J. Exp. Med.* 171:115.
8 Chatelain, R., Varkila, K. and Coffman, R. L. 1992. IL-4 induces a Th2 response in *Leishmania major*-infected mice. *J. Immunol.* 148:1182.
9 Julia, V. and Glaichenhaus, N. 1999. CD4$^+$ T cells which react to the *Leishmania major* LACK antigen rapidly secrete interleukin-4 and are detrimental to the host in resistant B10.D2 mice. *Infect. Immun.* 67:3641.
10 Guery, J. C., Galbiati, F., Smiroldo, S. *et al.* 1997. Non-MHC-linked Th2 cell development induced by soluble protein administration predicts susceptibility to *Leishmania major* infection. *J. Immunol.* 159:2147.

11 Kelly, B. L. and Locksley, R. M. 2004. The *Leishmania major* LACK antigen with an immunodominant epitope at amino acids 156 to 173 is not required for early Th2 development in BALB/c mice. *Infect. Immun.* 72:6924.

12 Noben-Trauth, N., Kropf, P. and Muller, I. 1996. Susceptibility to *Leishmania major* infection in interleukin-4-deficient mice. *Science* 271:987.

13 Shinkai, Y., Rathbun, G., Lam, K. P. *et al.* 1992. RAG-2-deficient mice lack mature lymphocytes owing to inability to initiate V(D)J rearrangement. *Cell* 68:855.

14 Suzue, K., Reinherz, E. L. and Koyasu, S. 2001. Critical role of NK but not NKT cells in acute rejection of parental bone marrow cells in F1 hybrid mice. *Eur. J. Immunol.* 31:3147.

15 Titus, R. G., Marchand, M., Boon, T. *et al.* 1985. A limiting dilution assay for quantifying *Leishmania major* in tissues of infected mice. *Parasite Immunol.* 7:545.

16 Moll, H., Flohe, S. and Rollinghoff, M. 1995. Dendritic cells in *Leishmania major*-immune mice harbor persistent parasites and mediate an antigen-specific T cell immune response. *Eur. J. Immunol.* 25:693.

17 Konecny, P., Stagg, A. J., Jebbari, H. *et al.* 1999. Murine dendritic cells internalize *Leishmania major* promastigotes, produce IL-12 p40 and stimulate primary T cell proliferation *in vitro*. *Eur. J. Immunol.* 29:1803.

18 von Stebut, E., Belkaid, Y., Jakob, T. *et al.* 1998. Uptake of *Leishmania major* amastigotes results in activation and interleukin 12 release from murine skin-derived dendritic cells: implications for the initiation of anti-*Leishmania* immunity. *J. Exp. Med.* 188:1547.

19 Banchereau, J. and Steinman, R. M. 1998. Dendritic cells and the control of immunity. *Nature* 392:245.

20 Shankar, A. H. and Titus, R. G. 1995. T cell and non-T cell compartments can independently determine resistance to *Leishmania major. J. Exp. Med.* 181:845.

21 Siegel, R. M., Katsumata, M., Komori, S. *et al.* 1990. Mechanisms of autoimmunity in the context of T-cell tolerance: insights from natural and transgenic animal model systems. *Immunol. Rev.* 118:165.

22 von Stebut, E., Belkaid, Y., Nguyen, B. V. *et al.* 2000. *Leishmania major*-infected murine langerhans cell-like dendritic cells from susceptible mice release IL-12 after infection and vaccinate against experimental cutaneous Leishmaniasis. *Eur. J. Immunol.* 30:3498.

23 Stober, D., Schirmbeck, R. and Reimann, J. 2001. IL-12/IL-18-dependent IFN-γ release by murine dendritic cells. *J. Immunol.* 167:957.

24 Gorham, J. D., Güler, M. L., Steen, R. G. *et al.* 1996. Genetic mapping of a murine locus controlling development of T helper 1/T helper 2 type responses. *Proc. Natl Acad. Sci. USA* 93:12467.

25 Gorham, J. D., Guler, M. L., Fenoglio, D. *et al.* 1998. Low dose TGF-β attenuates IL-12 responsiveness in murine Th cells. *J. Immunol.* 161:1664.

26 Shibuya, K., Robinson, D., Zonin, F. *et al.* 1998. IL-1α and TNF-α are required for IL-12-induced development of Th1 cells producing high levels of IFN-γ in BALB/c but not C57BL/6 mice. *J. Immunol.* 160:1708.

27 von Stebut, E., Ehrchen, J. M., Belkaid, Y. *et al.* 2003. Interleukin 1α promotes Th1 differentiation and inhibits disease progression in *Leishmania major*-susceptible BALB/c mice. *J. Exp. Med.* 198:191.

28 Sato, N., Ahuja, S. K., Quinones, M. *et al.* 2000. CC chemokine receptor (CCR)2 is required for langerhans cell migration and localization of T helper cell type 1 (Th1)-inducing dendritic cells. Absence of CCR2 shifts the *Leishmania major*-resistant phenotype to a susceptible state dominated by Th2 cytokines, B cell outgrowth, and sustained neutrophilic inflammation. *J. Exp. Med.* 192:205.

29 Guler, M. L., Gorham, J. D., Dietrich, W. F. *et al.* 1999. Tpm1, a locus controlling IL-12 responsiveness, acts by a cell-autonomous mechanism. *J. Immunol.* 162:1339.

30 Biedermann, T., Zimmermann, S., Himmelrich, H. *et al.* 2001. IL-4 instructs TH1 responses and resistance to *Leishmania major* in susceptible BALB/c mice. *Nat. Immunol.* 2:1054.

31 Kuroda, E., Sugiura, T., Zeki, K. *et al.* 2000. Sensitivity difference to the suppressive effect of prostaglandin E2 among mouse strains: a possible mechanism to polarize Th2 type response in BALB/c mice. *J. Immunol.* 164:2386.

PI3K is a negative regulator of IgE production

Tomomitsu Doi[1,2,4], **Kunie Obayashi**[1,5], **Takashi Kadowaki**[2,3], **Hideki Fujii**[1,2] and **Shigeo Koyasu**[1,2]

[1]Department of Microbiology and Immunology, Keio University School of Medicine, 35 Shinanomachi, Shinjuku-ku, Tokyo 160-8582, Japan
[2]Core Research for Evolutional Science and Technology, Japan Science and Technology Agency, Saitama, Japan
[3]Department of Metabolic Diseases, Graduate School of Medicine, University of Tokyo, Tokyo, Japan

[4]Present address: Department of Immunology and Genomic Medicine, Kyoto University Graduate School of Medicine, Yoshida Konoe-cho, Sakyo-ku, Kyoto 606-6501, Japan
[5]Present address: Department of Pharmacology, Kyoto University Graduate School of Medicine, Yoshida Konoe-cho, Sakyo-ku, Kyoto 606-6501, Japan

Abstract

The production of IgE, a main player in allergic disorders such as asthma and atopic dermatitis, is strictly regulated and the serum concentrations of IgE are normally kept at a much lower level than other isotypes. We found that mice deficient for the p85α regulatory subunit of class IA phosphoinositide 3-kinase (PI3K) produced increasing amounts of serum IgE. Purified p85$\alpha^{-/-}$ B cells produced more IgE than wild-type B cells *in vitro* in response to anti-CD40 mAb and IL-4. PI3K inhibitors wortmannin and IC87114 enhanced IgE production by wild-type B cells stimulated with anti-CD40 mAb and IL-4. Under the same condition, antigen receptor cross-linking induced the expression of inhibitor of differentiation-2 and suppressed the expression of activation-induced cytidine deaminase and class switch recombination (CSR) in a PI3K-dependent manner. IgE production was also suppressed in a concentrated cell culture condition, which was completely reversed by PI3K inhibition. The selective suppression of IgE production by PI3K was also observed at a protein level after CSR. Our results indicate that PI3K negatively regulates IgE production at both CSR and protein levels.

Introduction

IgE is involved in a defense mechanism against nematode, but at the same time, it is also a main player in allergic disorders such as asthma and atopic dermatitis (1). In normal circumstances, IgE production is strictly regulated and its serum concentration is much less than other isotypes (1). Although IgE has a relatively short half-life in plasma (2), it has been believed that the maintenance of low concentration of plasma IgE is ascribed to a tight control of IgE class switch recombination (CSR) (3, 4).

CSR takes place between two S regions located 5' to each constant region of Ig heavy chain (C_H) gene. The regulation of CSR in B cells was collaborated with the germ line transcription (GLT) of C_H genes and the induction of activation-induced cytidine deaminase (AID) expression. The specificity of C_H switch is regulated at the level of C_H GLT (5). IgE CSR is controlled by several molecules, the action of which converges on the regulation of Cε GLT that is induced by T_h2 cytokines IL-4 and IL-13 (6) and inhibited by a T_h1 cytokine IFN-γ (7). Therefore, T_h1/T_h2 balance is a critical factor for IgE production.

Several transcription factors are known to regulate the balance between T_h1/T_h2 differentiation. Those include GATA3 (8), which promotes T_h2 cell differentiation and inhibits T_h1 cell differentiation, and T-bet (9), which exerts the opposite effects to GATA3. In addition, IL-21 blocks IgE production from LPS-stimulated B cells by inhibiting Cε GLT (10). Several B cell surface receptors, including the B cell receptor (BCR) (11), CD45 (12), cytotoxic T lymphocyte antigen 4 (13) and transcription factors such as Bcl-6 (14) and inhibitor of differentiation-2 (Id2) (15), seem to inhibit this process as well. Furthermore, low-affinity IgE receptor CD23 suppresses IgE production by an unknown mechanism (2, 16). Since IgG1 CSR is also regulated by IL-4 (17), if the efficiency of IgG1 and IgE CSR are the same, IgE-expressing cells must exceed IgG1-expressing cells because IgG1-expressing cells subsequently switch to IgE-expressing cells (18–20). However, as mentioned, IgE production is controlled at a much lower rate than IgG1 production.

Phosphoinositide 3-kinases (PI3Ks) are lipid kinases that phosphorylate inositol phopholipids at the 3'-OH of inositol ring, generating second messengers that provide a binding

---

site for pleckstrin homology domains of many signaling molecules (21). The PI3K family is divided into four groups (IA, IB, II and III) according to their structural characteristics and substrate specificity. Class IA PI3Ks are dimers containing one of regulatory subunits, p85α, p55α, p50α, p85β, p55γ and one of catalytic subunits, p110α, p110β and p110δ. p85α is the most abundantly and ubiquitously expressed regulatory subunit of class IA PI3K. We and others previously reported that in mice deficient for the p85α, the number of mature B cells were reduced and the proliferation of peripheral B cells in response to BCR and LPS was severely impaired (22, 23). In addition, p85α$^{-/-}$ mice exhibit reduced production of T$_h$2 cytokines and enhanced production of T$_h$1 cytokines upon microbial infection (24, 25).

We demonstrate here that p85α$^{-/-}$ B cells produce more IgE than wild-type B cells and p85α$^{-/-}$ mice have increasing amounts of serum IgE despite the T$_h$1-biased immune responses. The inhibition of p110δ, a major catalytic subunit in B cells, enhances IgE production. In addition to the inhibition of IgG1 and IgE CSR, PI3K also suppresses IgE production at a protein level. Our results indicate that PI3K is an isotype selective negative regulator for IgE production.

Methods

Reagents and antibodies

FITC-anti-IgE, biotin-anti-IgG1, biotin-anti-IgG3, PE-anti-CTLA-4 antibodies and streptavidin–allophycocyanin were purchased from BD Biosciences (San Jose, CA, USA). Propidium iodide and carboxyfluoroscein succinimidyl ester (CFSE) were purchased from Sigma (St Louis, MO, USA). Anti-trinitrophenol–IgE was produced as ascites from a hybridoma and concentration was determined by ELISA. Anti-CD19 Magnetic Cell Sorting (MACS) beads were purchased from Miltenyi Biotec (Bergisch, Gladbach Germany). Anti-CD40 antibody was purchased from eBioscience (San Diego, CA, USA). Recombinant IL-4, IFN-γ and IL-21 were purchased from Peprotech (London, UK). Anti-IgM antibody F(ab)'$_2$ fragment was purchased from Jackson ImmunoResearch (Bar Harbor, ME, USA).

Mice and immunization

p85α$^{-/-}$ mice (22) on a C57BL/6 background were maintained under specific pathogen-free conditions at Taconic (Germantown, NY, USA) or our animal facility. p85α$^{-/-}$ and p85α$^{+/-}$ mice were obtained by intercrossing heterozygous (p85α$^{+/-}$) female mice with homozygous (p85α$^{-/-}$) male mice and littermate mice were used for each experiment. C57BL/6 mice were obtained from Sankyo Laboratory Service Company (Tokyo, Japan). All animal experiments were performed in accordance with our institutional guidelines. Mice were immunized intraperitoneally with 100 μg of (4-hydroxy-3-nitrophenyl) acetyl (NP)-conjugated chicken γ globulin (CGG) (NP-CGG) precipitated with alum or 5 μg of NP-CGG mixed with a CpG-based ImmunEagy mouse adjuvant (Qiagen) and boosted with 50 μg of soluble NP-CGG 71 days after primary immunization.

Immunohistochemistry

Tissue samples from spleen from immunized mice were frozen in Tissue-Tek O.C.T. compound (Sakura Finetechnical).

Tissue sections (6 μm thick) were prepared and fixed in acetone for 10 min. Endogenous peroxidase was blocked with 0.3% H_2O_2 in PBS for 10 min. Cells were stained with biotin-conjugated peanut agglutinin and streptavidin–HRP and counterstained with hematoxylin.

B cell purification and cell culture

Single cell suspensions of spleen cells were prepared, and red blood cells were removed by hypotonic lysis. B cells were purified with anti-CD19 magnetic beads using Auto-MACS (Miltenyi Biotec). Alternatively, splenocytes were incubated with FITC-anti-IgE, FITC-anti-CD11c, PE-anti-CD3ε, PE-anti-Gr-1 antibodies followed by anti-FITC and anti-PE magnetic beads and naive B cells were purified by Auto-MACS with a negative selection procedure according to the manufacturer's recommendation. The purity of splenic B cells and naive B cells were 95% and 85%, respectively. Essentially same results were obtained by both preparations. One hundred thousand B cells were cultured in one well of 96-well plates with 200 μl of complete medium (RPMI 1640 containing 10% FCS, sodium pyruvate, non-essential amino acid, penicillin and streptomycin) unless otherwise stated. For IgG1 and IgE CSR, B cells were stimulated with 5 μg ml^{-1} anti-CD40 antibodies and 10 ng ml^{-1} IL-4 for 4 days. For IgG3 CSR, cells were stimulated with 5 μg ml^{-1} anti-CD40 and 10 μg ml^{-1} LPS for 5 days.

Flow cytometric analysis

PBS containing 0.5% BSA and 10 mM ethyleneglycol-bis(2-aminoethylether)-N,N,N',N'-tetraacetic acid (EGTA) was used for staining except for the experiment shown in Fig. 1D where EGTA was omitted. Since secreted IgE binds B cell surface via CD23, EGTA treatment that removes bound IgE from CD23 is important to quantitate surface IgE expression. Cells were stained with biotin-anti-IgG1 or anti-IgG3 antibodies in 50% of normal rat serum. After washing, cells were stained with FITC–anti-IgE antibody and streptavidin–allophycocyanin. For intracellular staining, cells were fixed and permeabilized in 70% ethanol and stained with FITC–anti-IgE antibody.

ELISA and ELISPOT

NP-specific antibody titers were determined by ELISA using microtiter plates coated with NP-BSA. NP-BSA-coated plates were incubated with 1% BSA for blocking non-specific biding, and diluted serum samples were added to individual wells. Bound antibodies were revealed by HRP-conjugated anti-IgG1, IgG2a, IgM (SouthernBiotech, Birmingham, AL, USA) or IgE (Bethyl, Montgomery TX, USA) antibodies.

The frequency of IgE-producing cells was determined by enzyme-linked immunospot (ELISPOT) using anti-IgE antibody-coated filter plates. B cells (10^5 or 10^6) were plated in one well with culture medium. Plates were incubated at 37°C in a CO_2 incubator for 5 h. Spots derived from IgE-producing cells were visualized with HRP-conjugated anti-IgE antibody.

Reverse transcription–PCR and digestion circularization–PCR

Total RNA was purified with Trizol reagent (Invitrogen, San Diego, CA, USA). Two micrograms of total RNA was used
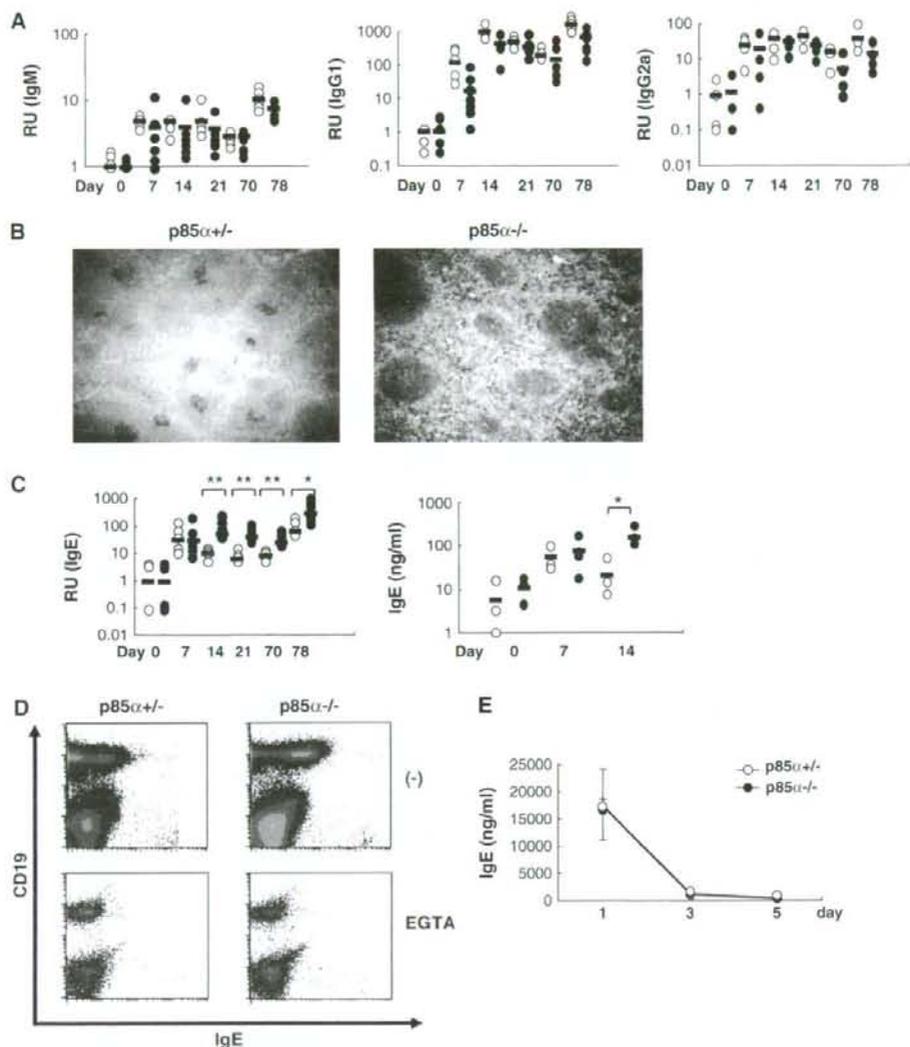
Fig. 1. Enhanced IgE production in p85α⁻/⁻ mice. Mice were immunized with alum-precipitated NP-CGG and boosted with soluble NP-CGG after 71 days. Open and filled circles in (A) and (C) show the titers of p85α⁺/⁻ (n = 6), p85α⁻/⁻ mice (n = 7), respectively. (A) NP-specific IgM, IgG1 and IgG2a responses were measured by ELISA. RU; relative unit. (B) Spleen sections from immunized p85α⁺/⁻ and p85α⁻/⁻ naive mice. Cells were stained with peanut agglutinin and hematoxylin. Brown is PNA. (C) NP-specific IgE (left) and total IgE (right) were measured by ELISA. **P < 0.01, *P < 0.05. (D) Splenocytes from p85α⁺/⁻ and p85α⁻/⁻ naive mice were stained with anti-CD19 and anti-IgE with or without EGTA pre-treatment. (E) Three hundred micrograms of trinitrophenol-specific IgE was injected intravenously to p85α⁺/⁻ and p85α⁻/⁻ mice (n = 4). After 1, 3, 5 days, serum trinitrophenol-specific IgE concentrations were measured by ELISA. Open and filled circles show the IgE titer of p85α⁺/⁻ and p85α⁻/⁻ mice, respectively.

for reverse transcription. The amounts of mRNAs for AID, Cγ1-GLT, γ1-circle transcript (CT), Cε-GLT, Iμ-Cε-post-switch transcript (PST), Id2 and β-actin were measured by semi-quantitative PCR. Digestion circularization (DC)–PCR was previously described (7, 26). Briefly, genomic DNA was digested with EcoRI. Self-ligated DNA fragments were used for PCR. PCR was done with the following primer pairs: AID, CAATTTT-CAGATCGCGTCCCT and GCGCTTTGCTCCTTTCTCTACA;

γ1-CT, GGCCCTTCCAGATCTTTGAG and AATGGTGCTGGG-CAGGAAGT; Cγ1-GLT, GGCCCTTCCAGATCTTTGAG and GGATCCAGAGTTCCAGGTCACT; Cε-GLT, CATCTGGGCAT-GAATTAATGGTTACTA and GTAGCTCCAAGGTGGGCTCAGT; Id2, CAGCCATTTCACCAGGAGAACA and CAGCATTCAG-TAGGCTCGTGTCA; Iμ-Cε-PST, CTCTGGCCCTGCTTATTGT-TG and GTAGCTCCAAGGTGGGCTCAGT; β-actin, GTGGGC-CGCTCTAGCCACCAA and TCTTTGATGTCACGCACGATTTC;

nAChR DC-PCR, GGCCGGTCGACAGGCGCGCACTGACAC-
CACTAAG and GCGCCATCGATGGACTGCTGTGGGTTTCAC-
CCAG; Sμ-Sγ1 DC-PCR, GGCCGGTCGACGGAGACCAA-
TAATCAGAGGGAAG and GCGCCATCGATGGAGAGCAGG-
GTCTCCTGGGTAGG and Sμ-Sε DC-PCR, GTCCTTCAATTT-
CTTACATAACC and ATGCAGGATACACCCCAGAC.

Statistics

We used Mann–Whitney's *U*-test for statistical analysis of
in vivo experiments and unpaired Student's *t*-test for statisti-
cal analysis of *in vitro* experiments.

Results

Enhanced IgE production in p85α⁻/⁻ mice

To investigate antibody response to T cell-dependent antigen in
p85α⁻/⁻ mice, mice were immunized with alum-precipitated
NP-CGG and boosted with soluble NP-CGG on day 71. NP-
specific IgM, IgG1, IgG2a and IgE titers were analyzed by
ELISA (Fig. 1). In p85α⁻/⁻ mice, IgM, IgG1 and IgG2a
responses to NP were comparable to or slightly less than those
of p85α⁺/⁻ mice (Fig. 1A). Germinal center formation after
immunization was impaired in p85α⁻/⁻ mice compared with
wild-type mice (Fig. 1B). These results are consistent with our
previous observation that mature B cell numbers are reduced
in p85α⁻/⁻ mice and BCR- and LPS-mediated activation is
partially impaired in p85α⁻/⁻ B cells (22).

Unexpectedly, p85α⁻/⁻ mice produced significantly more
NP-specific IgE than p85α⁺/⁻ mice from 14 days after immu-
nization and the higher titers were sustained for up to 70
days (Fig. 1C, left panel). Upon the secondary immunization
with soluble NP-CGG, the concentration of NP-specific se-
rum IgE was increased and the titers were higher in p85α⁻/⁻
than p85α⁺/⁻ mice. Total serum IgE of p85α⁻/⁻ mice was
also higher than that of p85α⁺/⁻ mice at 14 days after immu-
nization (Fig. 1C, right panel). These results indicate that the
lack of p85α leads to higher IgE response. Since alum is
a strong inducer of T cell-independent IL-4 production (27),
CpG-based adjuvant was used to examine if enhancement
of IgE production is due to alum-based immunization.
Although CpG-based adjuvant barely induced IgE in p85α⁺/⁻
mice, the adjuvant strongly induced IgE production in
p85α⁻/⁻ mice (data not shown), further demonstrating that
the lack of p85α results in a higher IgE response.

Before immunization, serum IgE titer was extremely low
and close to or below detection sensitivity because free IgE
is trapped by tissue mast cells and B cells via the high-affinity
IgE receptor FcεRI and the low-affinity IgE receptor CD23,
respectively. When B cells from unimmunized mice were
stained with anti-IgE antibody, substantial amounts of IgE
were detected on the surface of most splenic B cells from
p85α⁻/⁻ mice, while only low amounts were detected on B
cells from p85α⁺/⁻ mice (Fig. 1D). Such surface IgE was re-
moved by treating cells with EGTA, confirming that these
IgE molecules bound B cells via CD23. These results indi-
cate that p85α⁻/⁻ mice produce more IgE than p85α⁺/⁻ mice
even under naive conditions.

Since IgE is rapidly cleared from the serum compared with
other isotypes, it is possible that IgE clearance is impaired

in p85α⁻/⁻ mice. To test this possibility, IgE was exogenously
injected to p85α⁺/⁻ and p85α⁻/⁻ mice and serum IgE concen-
trations were measured (Fig. 1E). There was no difference in
the kinetics of IgE clearance between p85α⁺/⁻ and p85α⁻/⁻
mice. These results collectively indicate that IgE production is
accelerated in p85α⁻/⁻ mice without changing IgE clearance
from the serum.

Enhanced IgE production by p85α⁻/⁻ B cells

To determine whether the dysregulation of IgE production in
p85α⁻/⁻ mice is B cell autonomous, splenic B cells from
p85α⁻/⁻ and p85α⁺/⁻ mice were stimulated with anti-CD40
and IL-4 to induce CSR to IgG1 and IgE *in vitro*. The
amounts of IgM and IgG1 produced by p85α⁻/⁻ B cells in
the supernatant were lower than or comparative to those of
p85α⁺/⁻ B cells. In contrast, the production of IgE from p85α⁻/⁻
B cells was higher than that of p85α⁺/⁻ B cells (Fig. 2A).
Flow cytometric analysis and ELISPOT assay also demon-
strated that higher percentage of B cells expressed IgE in
p85α⁻/⁻ B cells than p85α⁺/⁻ B cells (Fig. 2B and C). These
results indicate that p85α deficiency in B cells enhances
IgE production.

Kinase activity of PI3K is required for IgE suppression

The major catalytic subunit of class IA PI3K expressed in B
cells is p110δ and the lack of p85α, which stabilizes p110s
(28, 29), greatly reduced the expression of p110δ (30). To
determine whether the kinase activity of PI3K is required for
IgE suppression, PI3K was inhibited with pharmacological
inhibitors and cell surface expression of IgG1, IgG3 and IgE
was examined by flow cytometry (Fig. 3A). IC87114, a spe-
cific inhibitor of p110δ (31), enhanced the number of cells
expressing IgE but not those expressing IgG1 or IgG3,
indicating that PI3K activity is required for IgE-selective sup-
pression. It is possible that the high percentages of IgE-
positive cells are caused by the specific survival of IgE-positive
cells compared with B cells expressing other isotypes in the
presence of PI3K inhibitor. However, IC87114 treatment for
3 days increased absolute number of IgE-positive cells
(Fig. 3B) without affecting cell division as examined by the
dilution of fluorescence intensity of CFSE-labeled B cells
(Fig. 3C), confirming that the inhibition of PI3K enhances
IgE CSR rather than the selective survival or proliferation of
IgE-expressing B cells.

Inhibition of PI3K enhances CSR to IgE and IgG1

We next examined the mechanisms of enhanced IgE pro-
duction by inhibiting PI3K. First, CSR was assayed by DC–
PCR and it was revealed that the PI3K inhibitor enhanced
both IgE and IgG1 CSR induced by anti-CD40 and IL-4
(Fig. 4A), indicating that PI3K activity directly suppresses
IgE production by blocking IgE CSR. It has been known that
BCR signal suppresses IgE and IgG1 CSR (11). We then
tested the effect of PI3K inhibitor on the BCR-mediated sup-
pression of CSR. As shown in Fig. 4B, BCR cross-linking
suppressed IgE CSR at the Cε GLT level. Interestingly, the
same signal suppressed IgG1 CSR as examined by γ1-CT
but Cγ1-GLT was unaffected (Fig. 4B). CSR examined by
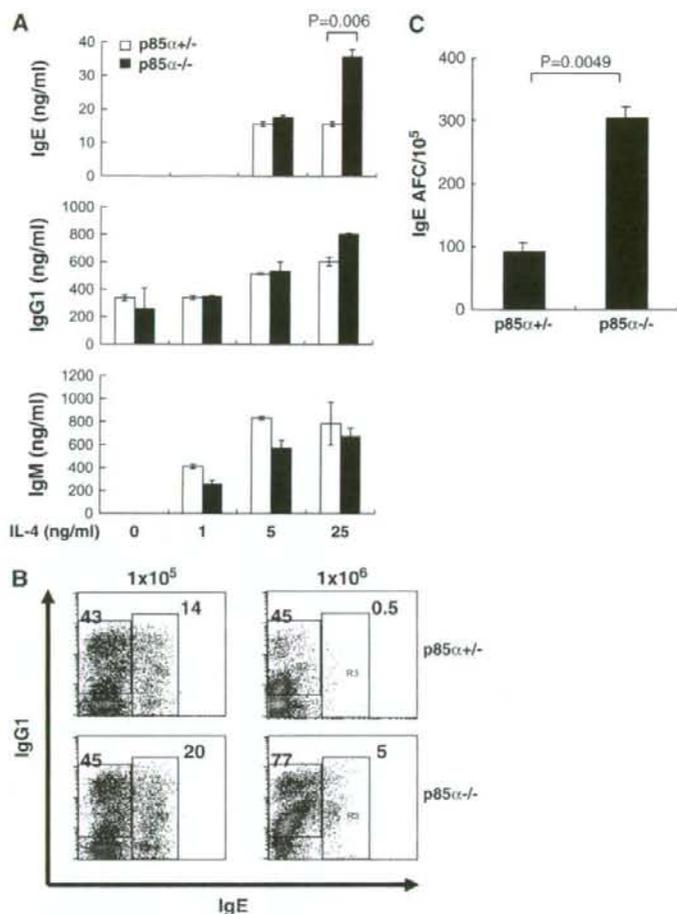
Fig. 2. Enhanced IgE production in p85α$^{-/-}$ B cells. (A) Purified splenic B cells were stimulated with 5 µg ml^{-1} anti-CD40 and indicated concentrations of IL-4. After 4 days, IgE, IgG1 and IgM titers in culture supernatants were measured by ELISA. White and black bars show the titers of p85α$^{+/-}$ and p85α$^{-/-}$ B cells, respectively. (B) The indicated numbers of p85α$^{+/-}$ and p85α$^{-/-}$ B cells were stimulated with 5 µg ml^{-1} anti-CD40 and 10 ng ml^{-1} IL-4 in 200 µl culture medium. The expression of IgG1 and IgE on the cell surface was analyzed by flow cytometry. The percentages of IgG1$^+$ and IgE$^+$ cells are indicated at each gate. (C) B cells were stimulated as in (A). The numbers of IgE-producing cells were counted by ELISPOT in duplicate cultures. Data are representatives of three independent experiments; data are shown as mean ± SD.

Cγ1-CT and Cε-GLT was partially recovered by wortmannin. Partial recovery of IgG1 CSR was confirmed by flow cytometric analysis (Fig. 4C). BCR signal also suppressed the expression of AID but induced Id2. Such inhibition of AID and induction of Id2 were partially reversed with PI3K inhibitor wortmannin, suggesting that PI3K is also involved in the BCR-mediated effects on CSR.

It is known that a T$_h$1 cytokine IFN-γ suppresses IgE production but IC87114 had no effect on IFN-γ-mediated suppression of IgE CSR (Fig. 4D). It has been reported that IL-21 specifically inhibits IgE CSR induced by a combination of LPS and IL-4 (10). However, IL-21 enhanced IgE CSR in B cells stimulated by a combination of anti-CD40 and IL-4. IC87114 treatment killed B cells in the presence of IL-21 (Fig. 4D).

PI3K-mediated cell density-dependent IgE suppression at post-translational level

It is known that IgE CSR is sensitive to cell density and IgE production is suppressed in high-density cell cultures (32). Enhanced IgE induction by p85α$^{-/-}$ B cells was more prominent in high-density cultures (Fig. 2B) as p85α$^{+/-}$ B cells were more sensitive to cell density than p85α$^{-/-}$ B cells. This observation prompted us to test the involvement of PI3K in cell density-dependent IgE suppression. IgE secretion and the percentages of IgE$^+$ cells decreased as cell density increased (Fig. 5A and B: thin lines). The inhibition of PI3K cancelled this suppression as IgE production became proportional to the cell numbers in the presence of IC87114 (Fig. 5A). In addition, the percentages of IgE$^+$ B cells were

A

B

C
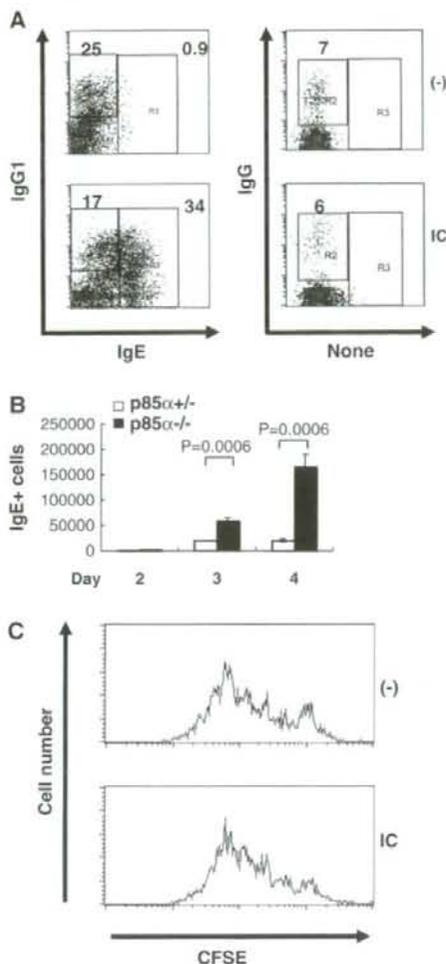
Fig. 3. The kinase activity of PI3K is required for IgE suppression. (A) Splenic B cells (1 × 10⁶ in 200 µl) were stimulated with 5 µg ml⁻¹ anti-CD40 and 10 ng ml⁻¹ IL-4 for IgG1 and IgE CSR, 5 µg ml⁻¹ anti-CD40 and 10 µg ml⁻¹ LPS for IgG3 CSR with (IC) or without (−) 5 µM IC87114. CSR was analyzed by flow cytometry. The percentages of B cells expressing IgG1, IgE, and IgG3 were indicated at each gate. (B) The absolute number of IgE⁺ cells at indicated days after stimulation. B cells were cultured in duplicate. Data are representatives of two independent experiments and are shown as mean ± SD. (C) CFSE-labeled B cells were cultured with anti-CD40 and IL-4 for 3 days in the presence (IC) or absence (−) of 5 µM IC87114. CFSE fluorescence intensities were analyzed by flow cytometry.

independent of cell density in the presence of IC87114 (Fig. 5B; thick lines). These results indicate that PI3K is involved in the cell density-dependent suppression of IgE production. Such density-dependent suppression was not observed for IgM and IgG1 secretion or IgM⁺ and IgG1⁺ cell numbers, indicating that the cell density-dependent suppression is specific for IgE production.

Even though IgE production was suppressed by high cell density, the amounts of IgE mRNA were unaffected by cell

density as examined by the amounts of Iµ-Cε-PST (Fig. 5C). When total IgE was stained by an intracellular staining method, it was revealed that the percentages of IgE-positive cells were not dramatically affected by cell density but the mean fluorescence intensity of IgE staining decreased as cell density increased (Fig. 5D), suggesting that the cell density-dependent inhibition of IgE is regulated at a protein synthesis, degradation and/or transport level. The inhibition of PI3K still elevated IgE amounts in high-cell density cultures compared with untreated cultures. These results collectively indicate that PI3K negatively regulates IgE production at both CSR and protein levels.

Discussion

Mast cells play a central role in allergic responses by releasing inflammatory substances. The activation of mast cells is triggered by the binding of allergen in complex with allergen-specific IgE to the high-affinity IgE receptors FcεRI. Since the pharmacological inhibition of p110δ reduced mast cell activation and protected mice against passive systemic anaphylactic allergic responses, p110δ was proposed to be a new target for therapeutic intervention in allergic diseases (33). As shown here, however, the inhibition of PI3K including p110δ augments IgE responses, raising the possibility that the inhibition of PI3K pathway *in vivo* may not be beneficial for the protection of allergic disorders. As demonstrated by the binding of higher amounts of IgE on p85α⁻/⁻ B cell surface via CD23 compared with those of wild-type B cells, the lack of p85α leads to higher level of IgE production even without immunization. In addition, we sometimes observed significant amounts of IgE in the serum of unimmunized p85α⁻/⁻ mice, indicating that IgE production is generally enhanced in the absence of p85α. Although it has been reported that the basal level of serum IgE in p110δ⁻/⁻ mice is comparable to that of wild-type mice (34), it will be of interest to examine the IgE response to exogenous antigen in those mice. *In vitro* induction of IgE CSR in p110δ⁻/⁻ B cells will also be informative to compare the phenotype observed in p85α⁻/⁻ mice in future studies.

Since the augmentation of IgE production by p85α⁻/⁻ B cells was reproduced by the inhibition of p110δ kinase activity with an isoform-specific inhibitor IC87114, it is likely that p85α suppresses IgE production by recruiting p110δ catalytic subunit rather than functioning as a GTPase activating protein (GAP) activity (35) that is independent of the kinase activity of PI3K. In addition, these results indicate that the PI3K activity in B cells autonomously regulates IgE production. It is of note that B cells deficient for phosphatase and tensin homolog deleted on chromosome 10 (PTEN), a negative regulator of PI3K, are unable to induce AID and CSR (36, 37), which is consistent with our observation. Downstream target of PI3K to suppress IgE production is elusive at the moment. BCR signal and cell–cell interaction must transduce signals through PI3K for IgE inhibition because CD40 and IL-4 receptor also activate PI3K via tumor necrosis factor receptor associated factor 6 (TRAF6) (38) and insulin receptor substrate 1 (IRS1) (39) molecules, respectively.

Our results demonstrate that PI3K negatively regulates IgE production through two different mechanisms. First
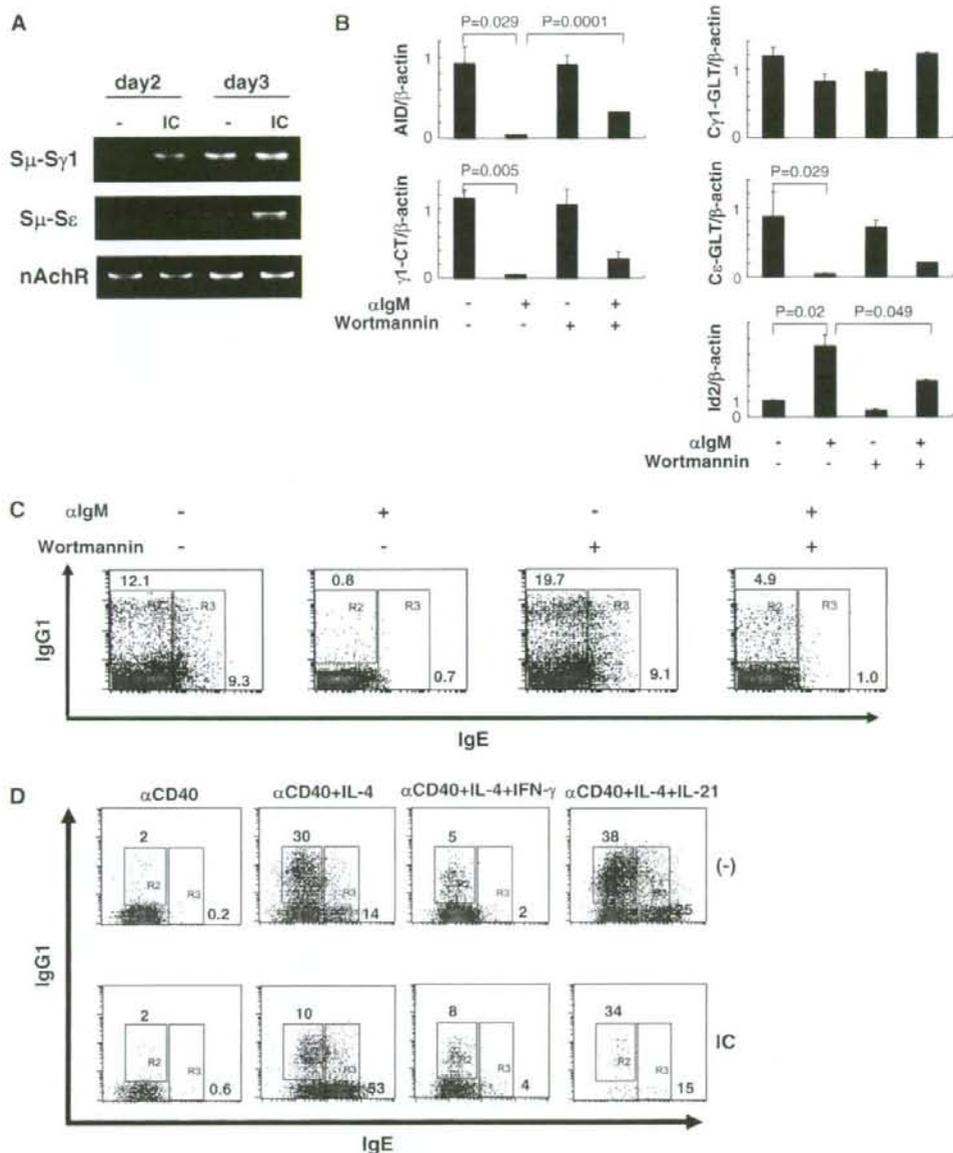
Fig. 4. BCR cross-linking inhibits IgG1 and IgE CSR via PI3K. B cells (1×10^5 in 200 μl) were stimulated with 5 μg ml^{-1} anti-CD40 and 10 ng ml^{-1} IL-4. (A) B cells were stimulated for 2 or 3 days with or without 5 μM IC87114. Sμ-Sγ1 and Sμ-Sε recombination was detected by DC–PCR. Nicotinic acetylcholine receptor (nAchR) was used as internal control for DC–PCR. (B) B cells were stimulated with or without 1 μg ml^{-1} anti-μ antibody with or without 100 nM of wortmannin for 2 days. The expression of β-actin, AID, γ1-CT, Cγ1-GLT, Cε-GLT and Id2 were measured by real-time PCR. PCR was done in duplicate and data are shown as mean ± SD. and representatives of three independent experiments are presented. (C) Splenic B cells were stimulated for 3 days with or without 100 nM wortmannin and the expression of IgG1 and IgE on the cell surface was analyzed by flow cytometry. (D) Flow cytometric analysis of stimulated B cells in the presence of 100 U ml^{-1} of IFN-γ or 20 ng ml^{-1} of IL-21 with or without 5 μM IC87114 for 4 days. The percentages of IgG1$^+$ and IgE$^+$ cells are indicated at each gate.

mechanism is the suppression of CSR for both IgG1 and IgE. It has been reported that the cross-linking of BCR inhibits CSR to IgG1 and IgE mediated by CD40 and IL-4 regardless of their effect on proliferation (11, 40) and the inhi-bition of PI3K partially restored the effect of BCR cross-linking (Fig. 4). In this context, it is of interest to note that high-dose allergen exposure specifically prevents IgE pro-duction and allergic responses (41–44). The mechanism of
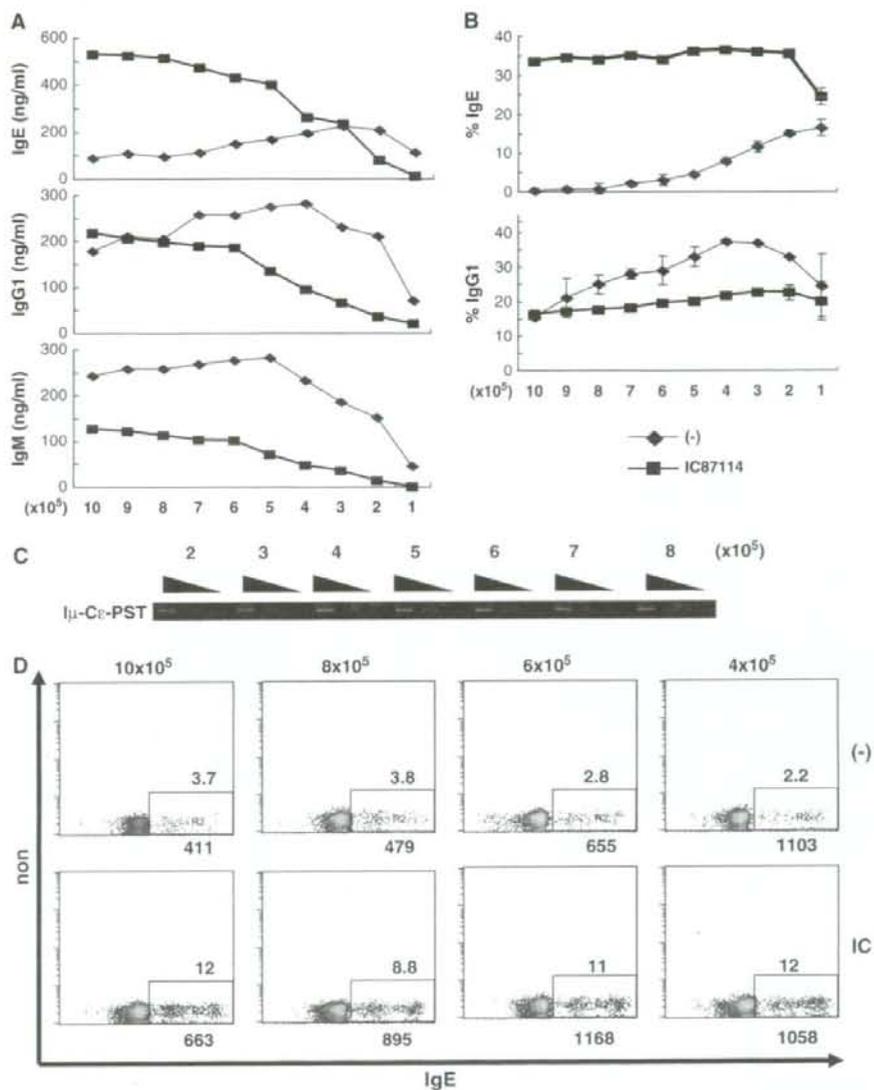
Fig. 5. Cell density-dependent IgE suppression is mediated by PI3K activity. The indicated concentrations of B cells were stimulated with 5 µg ml^{-1} anti-CD40 and 10 ng ml^{-1} IL-4 for 4 days with (square) or without (diamond) 5 µM IC87114. (A) The concentration of each isotype in the supernatant was measured by ELISA. (B) The percentages of IgE$^+$ and IgG1$^+$ were analyzed by flow cytometry. B cells were cultured in duplicate. Data are the mean ± SD. (C) The indicated numbers of cells were stimulated with 5 µg ml^{-1} anti-CD40 and 10 ng ml^{-1} IL-4 for 2 days. Iµ-Cε-PST was detected by reverse transcription–PCR. The amount of cDNA was normalized by β-actin. Five-fold serial dilutions of cDNAs were amplified. (D) The indicated numbers of cells were stimulated with (IC) or without (−) 5 µM of IC87114 for 4 days. Intracellular IgE was stained and analyzed by flow cytometry. The percentages of IgE$^+$ cells are indicated at each gate. The mean fluorescence intensities of IgE are indicated under each panel. Data are representatives of three independent experiments.

BCR-mediated CSR inhibition for IgE seems different from that for IgG1 as BCR cross-linking blocks Cε GLT but not Cγ1 GLT. BCR cross-linking induces the expression of Id2, which inhibits Cε-GLT (15) and, to a lesser extent, AID expression (45). While the block of AID induction results in the inhibition of IgG1 CSR in B cells stimulated by anti-CD40 and IL-4, IgE CSR is likely regulated at both AID induction and Cε GLT levels. As shown here, BCR-mediated Id2 induction was partially dependent on PI3K, implying the involvement of Id2 in the PI3K-mediated negative regulation of IgE CSR. Although Id2 is known to inhibit IgE CSR, Id2 is unlikely a main factor of PI3K-mediated IgE suppression

because IC87114 also enhanced IgE CSR in Id2$^{-/-}$ B cells (T. Doi, K. Obayashi and S. Koyasu, unpublished observation). In addition, it is known that IgE production is still lower than IgG1 in Id2$^{-/-}$ mice (15).

If the efficiency of IgG1 and IgE CSR is the same and IgG1 and IgE CSR occur independently, the percentages of IgG1-expressing cells must be lower than those of IgE-expressing cells because a part of IgG1-expressing cells subsequently switch to IgE-expressing cells (18–20). The fact that both IgG1 and IgE CSRs are negatively regulated by PI3K (Fig. 4A) yet the percentage of IgE-expressing cells is much lower than that of IgG1-expressing cells suggests the presence of another IgE-selective suppression mechanisms. Such second mechanism seems operative at the protein level as PI3K reduces IgE protein expression. It has previously been reported that IgE production is suppressed in a concentrated cell culture *in vitro* (32), which may explain the fact that IgE-expressing B cells are >1000 times more frequent in the nasal mucosa, which contain fewer B cells, than other lymphoid tissues (46). Our present results indicate that such density-dependent suppression is completely dependent on PI3K signaling (Fig. 5). The amount of IgE mRNA was not suppressed in high-density cultures, suggesting that the density-dependent suppression is controlled at a protein level. Although the mechanism is unclear at the moment, there are several possibilities. IgE expression may be suppressed at the level of protein synthesis, intracellular trafficking, internalization or degradation. Decrease of IgE$^+$ cells at high density may be due to internalization of IgE as has been shown for CTLA-4 in naive T cells (47). If this were the case, anti-IgE antibody added to the culture medium of IgE-expressing cells would accumulate inside the cells. To test this possibility, we compared the accumulation of FITC-conjugated anti-IgE antibody by IgE-expressing B cells at 37 or 4°C. No accumulation of anti-IgE antibody in B cells was observed after 3 h incubation at concentrated cell culture, while anti-CTLA-4 antibody accumulated in T cells at 37°C as reported (T. Doi, K. Obayashi and S. Koyasu, unpublished observation). Thus the lack of surface IgE is unlikely due to enhanced internalization. The total amount of IgE examined by intracellular staining was much lower in the absence of PI3K inhibitor than that in the presence of the inhibitor (Fig. 5). Therefore, PI3K-dependent degradation and/or block of IgE protein synthesis are more likely to explain IgE reduction at the protein level.

It has been reported that basal signal or tonic signal through BCR is critical for the survival of peripheral B cells and that B cells are eliminated from body shortly after BCR ablation (48). It is possible that PI3K-dependent suppression of surface IgE expression leads to the specific elimination of IgE-positive cells after IgE production, which should be examined in future studies.

Funding

Disclosures

Acknowledgements

Abbreviations

AID	activation-induced cytidine deaminase
BCR	B cell receptor
CGG	chicken γglobulin
CFSE	carboxyfluoroscein succinimidyl ester
CSR	class switch recombination
CT	circle transcript
DC	digestion circularization
GLT	germ line transcription
Id2	inhibitor of differentiation-2
NP	(4-hydroxy-3-nitrophenyl) acetyl
PI3K	phosphoinositide 3-kinase
PST	post-switch transcript

References

1 Geha, R., Jabara, H. and Brodeur, S. 2003. The regulation of immunoglobulin E class-switch recombination. *Nat. Rev. Immunol.* 3:721.
2 Yu, P., Kosco-Vilbois, M., Richards, M., Kohler, G. and Lamers, M. 1994. Negative feedback regulation of IgE synthesis by murine CD23. *Nature.* 369:753.
3 Snapper, C., Finkelman, F. and Paul, W. 1988. Differential regulation of IgG1 and IgE synthesis by interleukin 4. *J. Exp. Med.* 167:183.
4 Mao, C. and Stavnezer, J. 2001. Differential regulation of mouse germline Ig γ1 and ε promoters by IL-4 and CD40. *J. Immunol.* 167:1522.
5 Lutzker, S., Rothman, P., Pollock, R., Coffman, R. and Alt, F. 1988. Mitogen- and IL-4-regulated expression of germ-line Ig γ2b transcripts: evidence for directed heavy chain class switching. *Cell.* 53:177.
6 de Vries, J., Punnonen, J., Cocks, B., de Waal Malefyt, R. and Aversa, G. 1993. Regulation of the human IgE response by IL4 and IL13. *Res. Immunol.* 144:597.
7 Xu, L. and Rothman, P. 1994. IFN-γ represses ε germline transcription and subsequently down-regulates switch recombination to ε. *Int. Immunol.* 6:515.
8 Zheng, W. and Flavell, R. 1997. The transcription factor GATA-3 is necessary and sufficient for Th2 cytokine gene expression in CD4 T cells. *Cell.* 89:587.
9 Szabo, S., Kim, S., Costa, G., Zhang, X., Fathman, C. and Glimcher, L. 2000. A novel transcription factor, T-bet, directs Th1 lineage commitment. *Cell.* 100:655.
10 Suto, A., Nakajima, H., Hirose, K. *et al.* 2002. Interleukin 21 prevents antigen-induced IgE production by inhibiting germ line C(ε) transcription of IL-4-stimulated B cells. *Blood.* 100:4565.
11 Rush, J., Hasbold, J. and Hodgkin, P. 2002. Cross-linking surface Ig delays CD40 ligand- and IL-4-induced B cell Ig class switching and reveals evidence for independent regulation of B cell proliferation and differentiation. *J. Immunol.* 168:2676.

12 Yamada, T., Zhu, D., Saxon, A. and Zhang, K. 2002. CD45 controls interleukin-4-mediated IgE class switch recombination in human B cells through its function as a Janus kinase phosphatase. *J. Biol. Chem.* 277:28830.

13 Pioli, C., Gatta, L., Ubaldi, V. and Doria, G. 2000. Inhibition of IgG1 and IgE production by stimulation of the B cell CTLA-4 receptor. *J. Immunol.* 165:5530.

14 Harris, M., Chang, C., Berton, M. *et al.* 1999. Transcriptional repression of Stat6-dependent interleukin-4-induced genes by BCL-6: specific regulation of Iε transcription and immunoglobulin E switching. *Mol. Cell. Biol.* 19:7264.

15 Sugai, M., Gonda, H., Kusunoki, T., Katakai, T., Yokota, Y. and Shimizu, A. 2003. Essential role of Id2 in negative regulation of IgE class switching. *Nat. Immunol.* 4:25.

16 Sherr, E., Macy, E., Kimata, H., Gilly, M. and Saxon, A. 1989. Binding the low affinity FcεR on B cells suppresses ongoing human IgE synthesis. *J. Immunol.* 142:481.

17 Linehan, L., Warren, W., Thompson, P., Grusby, M. and Berton, M. 1998. STAT6 is required for IL-4-induced germline Ig gene transcription and switch recombination. *J. Immunol.* 161:302.

18 Yoshida, K., Matsuoka, M., Usuda, S., Mori, A., Ishizaka, K. and Sakano, H. 1990. Immunoglobulin switch circular DNA in the mouse infected with *Nippostrongylus brasiliensis*: evidence for successive class switching from μ to ε via γ1. *Proc. Natl Acad. Sci. USA.* 87:7829.

19 Mills, F., Thyphronitis, G., Finkelman, F. and Max, E. 1992. Ig μ-ε isotype switch in IL-4-treated human B lymphoblastoid cells. Evidence for a sequential switch. *J. Immunol.* 149:1075.

20 Siebenkotten, G., Esser, C., Wabl, M. and Radbruch, A. 1992. The murine IgG1/IgE class switch program. *Eur. J. Immunol.* 22:1827.

21 Koyasu, S. 2003. The role of PI3K in immune cells. *Nat. Immunol.* 4:313.

22 Suzuki, H., Terauchi, Y., Fujiwara, M. *et al.* 1999. *Xid*-like immunodeficiency in mice with disruption of the p85α subunit of phosphoinositide 3-kinase. *Science.* 283:390.

23 Fruman, D., Snapper, S., Yballe, C. *et al.* 1999. Impaired B cell development and proliferation in absence of phosphoinositide 3-kinase p85α. *Science.* 283:393.

24 Fukao, T., Tanabe, M., Terauchi, Y. *et al.* 2002. PI3K-mediated negative feedback regulation of IL-12 production in DCs. *Nat. Immunol.* 3:875.

25 Fukao, T., Yamada, T., Tanabe, M. *et al.* 2002. Selective loss of gastrointestinal mast cells and impaired immunity in PI3K-deficient mice. *Nat. Immunol.* 3:295.

26 Chu, C., Paul, W. and Max, E. 1992. Quantitation of immunoglobulin μ-γ1 heavy chain switch region recombination by a digestion-circularization polymerase chain reaction method. *Proc. Natl Acad. Sci. USA.* 89:6978.

27 Jordan, M., Mills, D., Kappler, J., Marrack, P. and Cambier, J. 2004. Promotion of B cell immune responses via an alum-induced myeloid cell population. *Science.* 304:1808.

28 Toker, A. and Cantley, L. 1997. Signalling through the lipid products of phosphoinositide-3-OH kinase. *Nature.* 387:673.

29 Katso, R., Okkenhaug, K., Ahmadi, K., White, S., Timms, J. and Waterfield, M. 2001. Cellular function of phosphoinositide 3-kinases: implications for development, homeostasis, and cancer. *Annu. Rev. Cell Dev. Biol.* 17:615.

30 Suzuki, H., Matsuda, S., Terauchi, Y. *et al.* 2003. PI3K and Btk differentially regulate B cell antigen receptor-mediated signal transduction. *Nat. Immunol.* 4:280.

31 Bilancio, A., Okkenhaug, K., Camps, M. *et al.* 2006. Key role of the p110δ isoform of PI3K in B-cell antigen and IL-4 receptor signaling: comparative analysis of genetic and pharmacologic interference with p110δ function in B cells. *Blood.* 107:642.

32 Rabah, D. and Conrad, D. 2002. Effect of cell density on *in vitro* mouse immunoglobulin E production. *Immunology.* 106:503.

33 Ali, K., Bilancio, A., Thomas, M. *et al.* 2004. Essential role for the p110δ phosphoinositide 3-kinase in the allergic response. *Nature.* 431:1007.

34 Okkenhaug, K., Bilancio, A., Farjot, G. *et al.* 2002. Impaired B and T cell antigen receptor signaling in p110δ PI 3-kinase mutant mice. *Science.* 297:1031.

35 Chamberlain, M., Berry, T., Pastor, M. and Anderson, D. 2004. The p85α subunit of phosphatidylinositol 3'-kinase binds to and stimulates the GTPase activity of Rab proteins. *J. Biol. Chem.* 279:48607.

36 Suzuki, A., Kaisho, T., Ohishi, M. *et al.* 2003. Critical roles of Pten in B cell homeostasis and immunoglobulin class switch recombination. *J. Exp. Med.* 197:657.

37 Omori, S., Cato, M., Anzelon-Mills, A. *et al.* 2006. Regulation of class-switch recombination and plasma cell differentiation by phosphatidylinositol 3-kinase signaling. *Immunity.* 25:545.

38 Arron, J., Vologodskaia, M., Wong, B. *et al.* 2001. A positive regulatory role for Cbl family proteins in tumor necrosis factor-related activation-induced cytokine (trance) and CD40L-mediated Akt activation. *J. Biol. Chem.* 276:30011.

39 Wang, L., Keegan, A., Paul, W., Heidaran, M., Gutkind, J. and Pierce, J. 1992. IL-4 activates a distinct signal transduction cascade from IL-3 in factor-dependent myeloid cells. *EMBO J.* 11:4899.

40 Cho, S. and Conrad, D. 1997. A new multivalent B cell activation model—anti-IgD bound to FcγRI: properties and comparison with CD40L-mediated activation. *Int. Immunol.* 9:239.

41 Sudowe, S., Rademaekers, A. and Kolsch, E. 1997. Antigen dose-dependent predominance of either direct or sequential switch in IgE antibody responses. *Immunology.* 91:464.

42 Arps, V., Sudowe, S. and Kolsch, E. 1998. Antigen dose-dependent differences in IgE antibody production are not due to polarization towards Th1 and Th2 cell subsets. *Eur. J. Immunol.* 28:681.

43 Sakai, K., Yokoyama, A., Kohno, N. and Hiwada, K. 1999. Effect of different sensitizing doses of antigen in a murine model of atopic asthma. *Clin. Exp. Immunol.* 118:9.

44 Riedl, M., Landaw, E., Saxon, A. and Diaz-Sanchez, D. 2005. Initial high-dose nasal allergen exposure prevents allergic sensitization to a neoantigen. *J. Immunol.* 174:7440.

45 Gonda, H., Sugai, M., Nambu, Y. *et al.* 2003. The balance between Pax5 and Id2 activities is the key to AID gene expression. *J. Exp. Med.* 198:1427.

46 Takhar, P., Smurthwaite, L., Coker, H. *et al.* 2005. Allergen drives class switching to IgE in the nasal mucosa in allergic rhinitis. *J. Immunol.* 174:5024.

47 Linsley, P., Bradshaw, J., Greene, J., Peach, R., Bennett, K. and Mittler, R. 1996. Intracellular trafficking of CTLA-4 and focal localization towards sites of TCR engagement. *Immunity.* 4:535.

48 Lam, K., Kuhn, R. and Rajewsky, K. 1997. *In vivo* ablation of surface immunoglobulin on mature B cells by inducible gene targeting results in rapid cell death. *Cell.* 90:1073.

ERK5 is involved in TCR-induced apoptosis through the modification of Nur77

Yasushi Fujii[1,2], Satoshi Matsuda[1,3,a], Gensuke Takayama[1] and Shigeo Koyasu[1,3,*]

[1]Department of Microbiology and Immunology, Keio University School of Medicine, 35 Shinanomachi, Shinjuku-ku, Tokyo 160-8582, Japan
[2]Department of Pediatrics, Keio University School of Medicine, 35 Shinanomachi, Shinjuku-ku, Tokyo 160-8582, Japan
[3]Core Research for Evolutional Science and Technology, Japan Science and Technology Agency, Tokyo 102-0081, Japan

Nur77 is a nuclear orphan steroid receptor that has been implicated in negative selection when immature T cells are strongly activated through interaction with self peptide-MHC complexes. The expression of Nur77 in thymocytes and T cell lines leads to apoptosis in a manner dependent on its transcriptional activity. It is well established that Nur77 function is negatively regulated by post-translational modification. Here we demonstrate that the MAPK-induced phosphorylation of Nur77 during T cell activation plays a critical role in the induction of apoptosis. Upon T cell receptor (TCR) stimulation, ERK5 (also known as big MAP kinase 1, BMK1), a member of the MAPK family, phosphorylates Nur77, leading to its transcriptional activation. In contrast, the activation of the ERK2 signaling pathway failed to activate Nur77 although ERK2 is also able to phosphorylate Nur77. Furthermore, the blockade of ERK5 signaling pathway suppressed TCR-induced cell death. These results indicate that ERK5 regulates Nur77 function through its phosphorylation.

Introduction

Apoptosis or programmed cell death is essential for the development and homeostasis of T cells. In the thymus, CD4^{+}CD8^{+} double positive (DP) thymocytes bearing T cell receptor (TCRs) that fail to recognize the self MHC molecules die rapidly through a process termed death by neglect, while the recognition of self MHC structures with bound peptide can trigger either functional differentiation (positive selection) or apoptosis (negative selection) of DP cells. If positively selected, immature DP thymocytes develop into mature single positive (SP) T cells expressing either CD4 or CD8. DP thymocytes bearing TCRs that strongly react with relatively abundant thymic self-antigens undergo negative selection, leading to the clonal deletion of potentially autoreactive T cells (von Boehmer 2004).

MAPK family members are evolutionarily conserved signaling molecules, which play a critical role in transducing extracellular signals to the nucleus. They include

ERK1/2, JNKs, p38 MAPKs and ERK5 (also termed big MAP kinase 1, BMK1) (Nishida & Gotoh 1993; Cobb & Goldsmith 1995; Schaeffer & Weber 1999). These pathways have significant roles in mediating signals triggered by cytokines, growth factors and environmental stresses, and are involved in proliferation, differentiation and apoptosis in many cell types. Several studies have demonstrated that intracellular signals through different MAPK cascades selectively regulate T cell development in the thymus: the ERK1/2 pathway is involved in positive selection and the p38 and/or JNK pathways in negative selection (Rincon et al. 1998; Sugawara et al. 1998; Diehl et al. 2000). It has also been reported that the duration and strength of ERK1/2 activation regulate both positive and negative selection (Mariathasan et al. 2001). However, the molecular targets of MAPK cascades during thymic selection remain obscure.

Nur77 (also known as NGFI-B in rat and TR3 in human), an orphan nuclear steroid receptor, plays a critical role in negative selection (Winoto & Littman 2002; Hsu et al. 2004). The expression of a dominant-negative Nur77 blocks activation-induced cell death in T-cell hybridomas as well as negative selection in the thymus of transgenic mice (Zhou et al. 1996). Conversely, transgenic mice that express wild-type Nur77 exhibit enhanced apoptosis and a reduction in both thymocyte numbers

and the proportion of DP thymocytes (Calnan *et al.* 1995). Thus, Nur77 likely plays an important role in T cell apoptosis.

TCR-mediated Nur77 expression requires an increase in intracellular calcium concentration (Woronicz *et al.* 1995). The Nur77 promoter has two calcium-regulated consensus binding sites for myocyte enhancer factor-2 (MEF2) (Woronicz *et al.* 1995). These observations implicate MEF2, originally discovered as a transcription factor for muscle-specific gene expression, as a calcium-dependent transcription factor for Nur77 expression. Recent findings further indicate that a TCR-induced increase in intracellular calcium concentration leads to the dissociation of MEF2 from Cabin1 as a result of the competitive binding of activated calmodulin to Cabin1, resulting in MEF2 binding to the Nur77 promoter (Youn *et al.* 1999). In addition to the calcium–MEF2 pathway, MAPK signaling pathways are also involved in the induction of Nur77 in excitable cells such as muscle and nerve cells (van den Brink *et al.* 1999; Sakaue *et al.* 2001). It is thus likely that Nur77 function is regulated through a MAPK pathway in addition to the MEF2 pathway during TCR-mediated apoptosis.

Here we demonstrate that Nur77 is phosphorylated through the ERK5 pathway. It has been shown that Akt-mediated phosphorylation of Nur77 inhibits its DNA binding activity (Masuyama *et al.* 2001). In contrast, ERK5-mediated phosphorylation is indispensable for the positive regulation of Nur77 function, as the inhibition of ERK5 pathway results in the blockade of TCR-mediated apoptosis. These results indicate that ERK5 plays an essential role in TCR-mediated apoptosis presumably through the post-translational modification of Nur77.

Results

Regulation of Nur77 function through its phosphorylation

TCR stimulation results in the activation-induced cell death of a murine T-cell hybridoma, DO11.10 cells (Liu *et al.* 1994; Woronicz *et al.* 1994). The same stimulation induced the transient expression of Nur77 in these cells (Fig. 1A) (Winoto & Littman 2002; Hsu *et al.* 2004). Similar to TCR stimulation, simultaneous stimulation with PMA and A23187 that can mimic TCR signals (Koyasu *et al.* 1987) induced Nur77 expression, reaching a peak at 3 h after stimulation (data not shown). The stimulation of cells with A23187 alone induced the expression of Nur77 to a level comparable to PMA and A23187 stimulation while stimulation with PMA alone failed to induce Nur77 expression (Fig. 1B, upper panel).
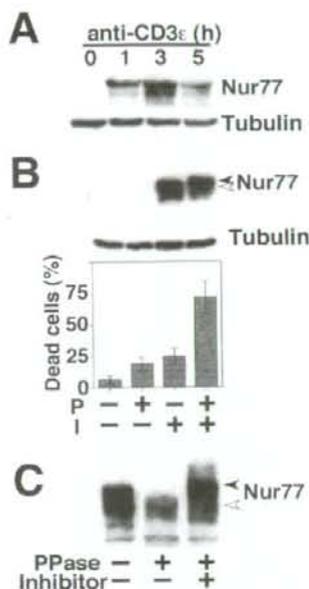
Figure 1 Nur77 is phosphorylated during T cell activation. (A) DO11.10 cells were stimulated with plate-bound anti-CD3ε (145-2C11) mAb for the indicated times. Cell lysates (corresponding to 2×10^6 cells) were then obtained and subjected to immunoblot analysis with an anti-Nur77 mAb (upper panel) or an anti-α-tubulin mAb (lower panel) as a loading control. (B) DO11.10 cells were stimulated with 5 ng/mL PMA (P) and/or 200 ng/mL A23187 (I) and subjected to immunoblot analysis using the anti-Nur77 mAb (3 h after stimulation, upper panel) or the anti-αtubulin mAb as a loading control (middle panel) as well as cell death assay by a dye-exclusion method (20 h after stimulation, lower panel). As for death assay, three independent experiments were performed and data are presented as means ± SD. Closed and open arrowheads indicate Nur77 bands corresponding to a slower migrating form and a faster migrating form, respectively. (C) DO11.10 cells were stimulated with 5 ng/mL PMA and 200 ng/ml A23187 for 3 h. The cell lysates were obtained without phosphatase inhibitors, followed by incubation with 50 U/mL calf intestine alkaline phosphatase (PPase) in the presence or absence of 100 mM β-glycerophosphate (Inhibitor) at 37 °C for 30 min. Closed and open arrowheads indicate Nur77 bands corresponding to a phosphorylated form and a non-phosphorylated form, respectively.

This is in line with the previous observation that the expression level of Nur77 is regulated through the Ca^{2+}-induced Cabin1–MEF2 pathway (Youn *et al.* 1999). To our surprise, however, treatment with A23187 alone caused apoptosis in DO11.10 cells only marginally, whereas simultaneous stimulation with PMA was required

to fully induce apoptosis (Fig. 1B, lower panel). It should be noted that the electrophoretic mobility of Nur77 is somewhat slower when stimulated with PMA and A23187 compared to stimulation with A23187 alone (compare lanes 3 and 4), raising the possibility that the PMA-induced modification of Nur77 is involved in its ability to cause apoptosis. Given that the phosphorylation status of proteins often affects their electrophoretic mobility, we examined whether Nur77 is phosphorylated during T cell activation. Nur77 induced via simultaneous stimulation with PMA and A23187 was incubated with alkaline phosphatase in the presence or absence of a phosphatase inhibitor. Treatment with alkaline phosphatase resulted in the disappearance of the more slowly migrating Nur77 protein bands while the addition of a phosphatase inhibitor to the reaction canceled the effect of alkaline phosphatase (Fig. 1C). These results strongly suggest that Nur77 is phosphorylated during T cell activation presumably through PMA-sensitive signaling pathways.

MAPK signaling pathway is responsible for Nur77 phosphorylation

Given that PMA treatment activates a variety of MAPK family members, we investigated the effects of MAPK inhibitors on PMA-induced Nur77 phosphorylation. Since p38 and/or JNK pathways are implicated in negative selection in the thymus (Rincon et al. 1998; Sugawara et al. 1998; Diehl et al. 2000), we initially expected that Nur77 phosphorylation would be suppressed in the presence of SB203580. Although SB203580 is a well-known inhibitor for p38, it has been reported that SB203580 is also able to inhibit JNK activity at a concentration higher than 10 μM (Chen et al. 1998). Contrary to our expectation, SB203580 had little effect on Nur77 phosphorylation during T cell activation (Fig. 2A). In contrast, the treatment of cells with PD98059 as well as U0126, both of which are well-known inhibitors for the ERK1/2 cascade (Pang et al. 1995; DeSilva et al. 1998), suppressed the phosphorylation of Nur77, which is demonstrated by disappearance of the slowly migrating bands (Fig. 2A).

As previously reported (Yazdanbakhsh et al. 1995), treatment with cyclosporin A (CsA), a potent inhibitor of the calcium–calcineurin pathway, led to the marked reduction of Nur77 expression (Fig. 2A). Interestingly, CsA had little effect on the phosphorylation status of Nur77 as demonstrated by the existence of the slowly migrating bands (Fig. 2B). At concentrations ranging from 2.5 to 10 μM, U0126 had, if any, a marginal effect on Nur77 expression while blocking Nur77 phosphorylation (Fig. 2B). However, Nur77 expression during T
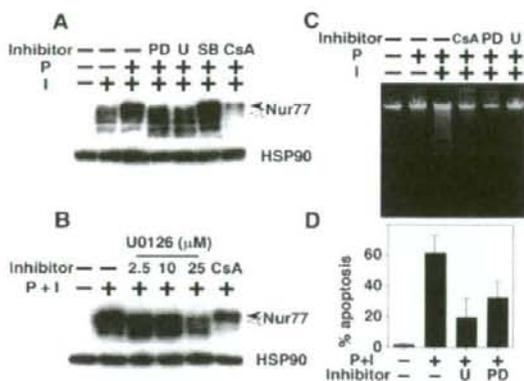
Figure 2 Effects of MAPK inhibitors on Nur77 phosphorylation. (A) DO11.10 cells were pretreated with 50 μM PD98059 (PD), 10 μM U0126 (U), 10 μM SB203580 (SB) or 100 ng/ml CsA for 1 h, followed by stimulation with 5 ng/mL PMA (P) and 200 ng/mL A23187 (I) for 3 h. Cell lysates were subjected to immunoblot analysis with the anti-Nur77 mAb (upper panel) and an anti-HSP90 antibody as a loading control (lower panel). Solid and open arrowheads indicate mobility of the bands corresponding to hyper- and hypo-phosphorylated Nur77, respectively. (B) DO11.10 cells were pretreated with U0126 at the indicated concentrations or 100 ng/mL CsA for 1 h, followed by stimulation with 5 ng/mL PMA and 200 ng/mL A23187 (P + I) for 3 h. The cells were subjected to immunoblot analysis with the anti-Nur77 mAb (upper panel) and the anti-HSP90 antibody as a loading control (lower panel). (C) DO11.10 cells were pretreated with 50 μM PD98059 (PD), 10 μM U0126 (U) or 100 ng/mL CsA for 1 h, followed by stimulation with 5 ng/mL PMA (P) and/or 200 ng/mL A23187 (I) for 10 h. The cells were then subjected to DNA fragmentation assay. (D) DO11.10 cells were pretreated with 10 μM U0126 (U) or 50 μM PD98059 (PD) for 1 h, followed by stimulation with 5 ng/mL PMA and 200 ng/mL A23187 (P + I) for 16 h. The percentages of apoptotic cells were then evaluated by annexin-V staining. Three independent experiments were performed and data are presented as means ± SD.

cell activation was partially inhibited in the presence of a higher concentration (25 μM) of U0126, suggesting that an U0126-sensitive signaling pathway(s) is also involved in the Nur77 expression (Fig. 2B). As shown in Fig. 2C, DNA fragmentation, an indicator of apoptosis, caused by simultaneous stimulation with PMA and A23187 was blocked by the pretreatment of cells with CsA. Moreover, pretreatment with either U0126 or PD98059 also led to nearly complete inhibition of DNA fragmentation under conditions where the expression level of Nur77 was maintained at a level comparable to that without inhibitors. The suppressive effect of U0126 as well as PD98059 on DO11.10 was confirmed by FACS analysis using annexin-V as an indicator for apoptosis (Fig. 2D).

Although PD98059 and U0126 are highly selective inhibitors of the ERK1/2 signaling pathway (Pang *et al.* 1995; DeSilva *et al.* 1998), the ERK5 signaling pathway is also sensitive to these reagents (Kamakura *et al.* 1999). This was indeed the case with DO11.10 cells (Fig. 3). Pretreatment of the cells with PD98059 suppressed both ERK2 and ERK5 activation in response to PMA and A23187. Furthermore, U0126 reduced ERK2 and ERK5 activation to a nearly basal level (Fig. 3A,B). When we compared the kinetics of ERK1/2 and ERK5 activation, we found that ERK5 activation was more sustained in comparison with ERK2 (Fig. 3A,C). We also noted that stimulation with PMA and A23187 failed to activate ERK1 in DO11.10 cells where ERK1 was expressed to a level comparable to ERK2 (Fig. 3A and data not shown). On the other hand, CsA had no effect on ERK2 or ERK5 activation while apoptosis was inhibited.

These data raise the possibility that the ERK5 and/or ERK2 signaling pathways are involved in Nur77 phosphorylation. Consistent with this idea, we found that mouse Nur77 contains 12 potential MAPK phosphorylation sites, which are evolutionarily conserved among mouse, rat and human species. Indeed, ERK5 as well as ERK2 directly phosphorylated recombinant mouse Nur77 protein *in vitro* (Fig. 3D). We thus examined whether ERK5 and/or ERK2 are able to phosphorylate Nur77 *in vivo* by using COS7 cells, which are resistant to Nur77-induced apoptosis, to avoid secondary effects caused by the apoptotic process. It is well established that MAPK is efficiently activated in the presence of its cognate upstream activator, MAPKK (Nishida & Gotoh 1993). The activation of either ERK2 (by co-transfection with ERK2 and ΔSESE, a constitutively active form of MEK1) or ERK5 (by co-transfection with ERK5 and MEK5(D), a constitutively active form of MEK5) led to Nur77 phosphorylation as demonstrated by the appearance of more slowly migrating bands (Fig. 3E). In contrast, the co-expression of inactive MEK1 (referred to here as SASA) and MEK5 (referred to here as MEK5(A)) failed to induce Nur77 phosphorylation. These results collectively indicate that ERK5 and ERK2 are capable of phosphorylating Nur77 *in vitro* and *in vivo*.

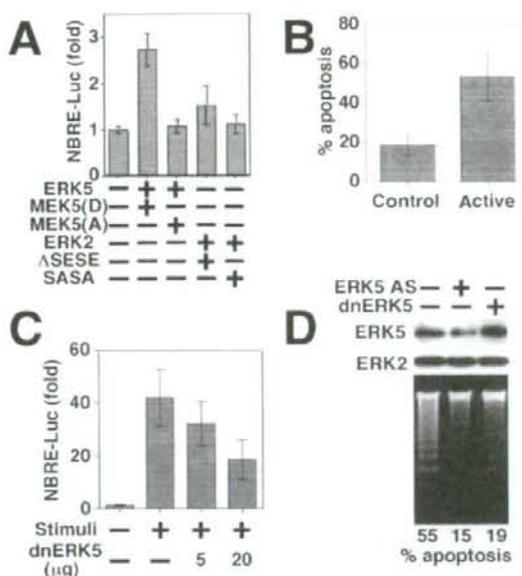## ERK5-mediated phosphorylation is important for Nur77 function

We next examined whether MAPK-mediated phosphorylation affects Nur77 function. Previous reports have demonstrated that the translocation of Nur77 to mitochondria results in cytochrome *c* release, which causes activation of the caspase 9/caspase 3 cascade and leads to apoptosis in some cell lines such as LNCaP cells (Li *et al.*
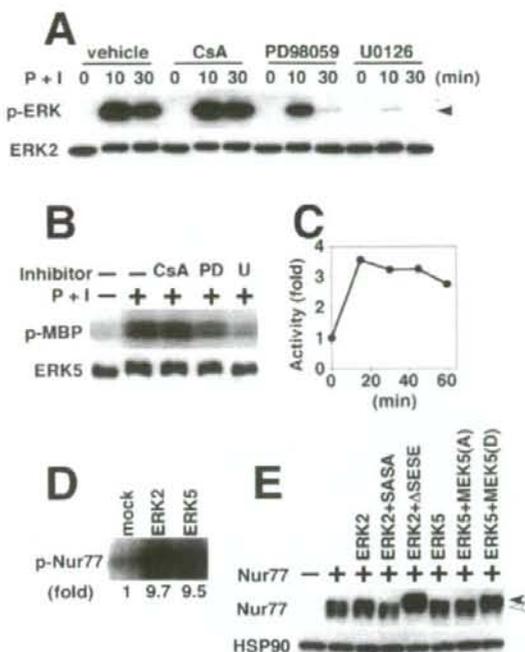
Figure 3 ERK5 as well as ERK2 signaling pathways are involved in Nur77 phosphorylation. (A) DO11.10 cells were pretreated with 100 ng/mL CsA, 50 μM PD98059 or 10 μM U0126 for 1 h, followed by stimulation with 5 ng/mL PMA and 200 ng/mL A23187 (P + I) for the indicated times. ERK1/2 activity was estimated by immunoblot analysis with an anti-phospho-ERK1/2 mAb. Closed and open arrowheads indicate positions corresponding to phosphorylated ERK2 and phosphorylated ERK1, respectively. (B) DO11.10 cells were pretreated with 100 ng/mL CsA, 50 μM PD98059 (PD) or 10 μM U0126 (U) for 1 h, followed by stimulation with 5 ng/mL PMA and 200 ng/mL A23187 (P + I) for 10 min. The cell lysates were then subjected to immunoprecipitation with an anti-ERK5 antibody, followed by an *in vitro* kinase assay using MBP as a substrate. (C) DO11.10 cells were stimulated with 5 ng/mL PMA and 200 ng/mL A23187 for the indicated times. The cell lysates were immunoprecipitated with an anti-ERK5 antibody, and assayed for ERK5 activity. This experiments is a representative of two. (D) DO11.10 cells were stimulated with 5 ng/mL PMA and 200 ng/mL A23187 for 10 min, followed by immunoprecipitation with a control IgG (mock), the anti-ERK2 antibody, and the anti-ERK5 antibody. The immunoprecipitates were incubated with GST-Nur77 in the presence of [γ-^{32}P] ATP, and ^{32}P incorporation was quantified on a BAS2000. (E) COS7 cells were transfected with an expression vector for GFP-fused Nur77 along with the indicated combination of MAPKK-MAPK. Cell lysates were obtained after 36-h incubation, and subjected to immunoblot analysis with an anti-GFP mAb (upper panel) and an anti-HSP90 antibody (lower panel). Closed and open arrowheads indicate Nur77 bands corresponding to a hyper-phosphorylated form and a hypo-phosphorylated form, respectively.

2000). However, TCR-induced Nur77 exclusively localized in the nucleus in DO11.10 cells (data not shown), which is consistent with a previous observation that the transcriptional activity of Nur77 correlated with its potential to cause apoptosis in T cells (Kuang et al. 1999). In addition, MAPK is known to translocate into the nucleus once activated (Cobb & Goldsmith 1995; Schaeffer & Weber 1999). It is thus likely that MAPK-mediated phosphorylation regulates the transcriptional activity of Nur77 in the nucleus. In fact, without MAPK-mediated phosphorylation, Nur77 had very low transcriptional activity whereas the activation of ERK5 pathway augmented the transcriptional activity of Nur77 (Fig. 4A). Interestingly, the activation of ERK2 pathway had a marginal effect on Nur77 activation. These data demonstrate that ERK5-mediated, but not ERK2-mediated phosphorylation is sufficient to activate Nur77. We also found that the activation of ERK5 pathway augmented A23187-induced apoptosis in DO11.10 cells (Fig. 4B). In addition, the expression of a dominant negative form of ERK5 (referred to here as dnERK5), which interferes the interaction between endogenous ERK5 and its substrate (Nakaoka et al. 2003), suppressed Nur77 activation induced by simultaneous stimulation with PMA and A23187 (Fig. 4C). It is thus likely that ERK5 plays a critical role in Nur77-mediated apoptosis, presumably through increasing transcriptional activity of Nur77. In silico analysis <http://mbs.cbrc.jp/research/db/TFSEARCH.html> suggests that Thr residue at 145 located within the transcriptional activation domain is a candidate for ERK5-mediated phosphorylation site. However, a mutant form of Nur77 where Ala was substituted for Thr 145 had similar transcriptional activity to wild-type Nur77 when over-expressed in DO11.10 cells (data not shown). The functional phosphorylation site(s) by ERK5 in Nur77 is now under investigation.

To examine whether the activation of ERK5 pathway is required for Nur77-induced apoptosis, we utilized a functional knockdown approach. Although Sohn et al. have reported the functional siRNA sequence for murine ERK5 (Sohn et al. 2005), we failed to reproduce their result via lentiviral vector-mediated introduction (data not shown). We thus chose more classical antisense approach to knockdown endogenous ERK5 in DO11.10 cells. Consistent with our expectation, the introduction of antisense ERK5 construct into DO11.10 cells reduced the expression level of endogenous ERK5, rendering the cells resistant to TCR-induced apoptosis (Fig. 4D, compare lanes 1 and 2). Furthermore, DO11.10 cells expressing dnERK5 were also resistant to TCR-induced apoptosis (Fig. 4D, compare lanes 2 and 3). We thus conclude that ERK5 is an essential component for Nur77-mediated T cell apoptosis.

Figure 4 ERK5-mediated phosphorylation of Nur77 is required to cause apoptosis. (A) DO11.10 cells were transfected with NBRE-luc and phRL-TK along with the indicated combination of MAPKK-MAPK. Luciferase activities were measured at 7 h after stimulation with 200 ng/mL A23187 according to the manufacturer's instructions (Promega). (B) DO11.10 cells were transfected with pEGFP alone (control) or MEK5(D) along with pEGFP-ERK5 (active). The cells were then stimulated with 200 ng/mL A23187 for 16 h. The percentages of apoptotic cells among GFP-positive cells were evaluated by annexin-V staining. Three independent experiments were performed and data are presented as means ± SD. (C) DO11.10 cells were transfected with NBRE-luc and phRL-TK along with or without the indicated amounts of the expression vector for dnERK5. Luciferase activities were measured at 7 h after stimulation with 5 ng/mL PMA and 200 ng/mL A23187. (D) DO11.10 cells were stably transfected with expression vectors for the indicated constructs. The expression level of ERK5 was indicated by immunoblot analysis with the anti-ERK5 antibody (upper panel) and the anti-ERK2 antibody served as loading control (middle panel). The transfectants were stimulated with plate-bound 145-2C11 for 12 h, and assayed for DNA fragmentation (lower panel). Shown are percentages of apoptotic cells evaluated by annexin-V staining at 16 h after stimulation.

Discussion

ERK5, also known as BMK1, is a member of the MAPK family and is activated by a wide range of extracellular stimuli such as mitogens (Kato et al. 1997, 2000; English et al. 1999; Kamakura et al. 1999) and stress (Abe et al.

1996). It has been shown that ERK5 plays a critical role in a variety of physiological processes such as the differentiation of skeletal muscle cells, cardiac development, vascular maturation/angiogenesis and neural differentiation (Dinev *et al.* 2001; Regan *et al.* 2002; Nishimoto *et al.* 2005). However, whether ERK5 is involved in the TCR signaling pathway has been obscure. The results presented here suggest that the phosphorylation of Nur77 presumably mediated through ERK5 signaling pathway is required for its function in causing apoptosis during T cell activation. It is of interest to note that one of the best-characterized substrates of ERK5 is MEF2C (Kato *et al.* 1997), which has been shown to be involved in TCR-induced Nur77 induction (Youn *et al.* 1999). Consistently, the blockade of ERK5 activation with a higher dose of U0126 resulted in the partial inhibition of Nur77 expression during T cell activation (Fig. 2B). Furthermore, it has been reported that the C-terminal domain of ERK5 when over-expressed augments Nur77 gene expression (Kasler *et al.* 2000). These results collectively suggest that the ERK5 pathway affects Nur77 function through two distinct mechanisms, gene expression and post-translational modification.

We hypothesize that the ERK5–Nur77 pathway functions as a signal integrator to quantify the strength of TCR engagement and direct the cell fate of immature T cells determining whether or not the cells will die. This concept is in line with an observation that Nur77 is induced even during positive selection where a weak signal is transduced into the nucleus (Masuyama *et al.* 2001). Interestingly, it has been shown that the pretreatment of fetal thymocytes with PD98059 resulted in the blockade of negative selection, leading to the conclusion that ERK1/2 pathways are involved in negative selection (Mariathasan *et al.* 2000). However, based on our observation, this could be explained by the inhibition of Nur77 function through suppressing ERK5 pathway in PD98059-treated cells. Studies with conditional knockout mice recently established (Hayashi *et al.* 2004) will clarify the contribution of the ERK5 pathway to negative selection under physiological conditions.

It is yet to be determined why ERK2 activation had only a slight effect on the transcriptional activation of Nur77 although the activation of ERK2 pathway resulted in Nur77 phosphorylation to a level comparable to the ERK5 pathway (Fig. 3D,E). One possible mechanism is that ERK5 activation is sustained while ERK2 activation is transient and such sustained activation of ERK5 is required for the post-translational modification of Nur77 (Fig. 3A,C) as is the case for c-Fos stabilization during IL-6/gp130 stimulation (Sasaki *et al.* 2006). Alternatively, since ERK5 and ERK2 phosphorylate distinct subsets of

transcription factors in the nucleus (Kamakura *et al.* 1999), it is possible that Nur77 phosphorylation mediated by ERK2, which may occur on a site(s) distinct from that phosphorylated by ERK5, rather inhibits Nur77 function. In accordance with this hypothesis, Katagiri *et al.* have reported that the activation of conventional Ras/MAPK cascade, which is presumably mediated through ERK1/2, resulted in the phosphorylation of Nur77 at Ser105, leading to nuclear export of Nur77 (Katagiri *et al.* 2000). This would be consistent with the observation demonstrating that the ERK1/2 pathway plays a critical role in positive selection (Sugawara *et al.* 1998): ERK1/2-mediated phosphorylation suppresses Nur77 function leading to survival and differentiation of DP cells.

In summary, present results show that ERK5 plays an important role in T cell apoptosis by enhancing the transcriptional activity of Nur77 through phosphorylation. Our results also suggest that ERK5 and ERK1/2 play distinct roles in the regulation of Nur77 and T cell fate during thymic development.

Experimental procedures

Cell culture and transfection

The DO11.10 mouse T-cell hybridoma (Haskins *et al.* 1983) and COS7 cells were maintained in RPMI 1640 medium containing 10% FCS, penicillin–streptomycin, 10 mM Hepes buffer solution and 50 μM β-mercaptoethanol (Invitrogen, Carlsbad, CA). For electroporation, DO11.10 cells (1×10^7) suspended in Opti-MEM (Invitrogen) were mixed with 25 μg of plasmid DNA, and electroporated with a 250-V pulse at 960 μF on a Gene Pulser apparatus (Bio-Rad, Hercules, CA). COS7 cells were transfected with Superfect transfection reagent (Qiagen, Valencia, CA) according to the manufacturer's instructions.

Antibodies and reagents

The antibodies and inhibitors used in this study include anti-Nur77 mAb (BD Bioscience, Franklin Lakes, NJ), anti-GFP mAb (Clontech, Palo Alto, CA), anti-ERK2 polyclonal antibody (Santa Cruz Biotechnology Inc., Santa Cruz, CA), anti-ERK5 polyclonal antibody and anti-αtubulin mAb (Sigma, St. Louis, MO), anti-phospho-ERK1/2 mAb and PD98059 (Cell Signaling, Beverly, MA), anti-HSP90 polyclonal antibody (Yonezawa *et al.* 1988), U0126 and SB203580 (Calbiochem, San Diego, CA). Anti-CD3ε mAb (145-2C11) was purified from the culture supernatant of a hybridoma 145-2C11. Phorbol-12-myristate 13-acetate (PMA) was purchased from Sigma, and calcium ionophore A23187 was from Calbiochem.

Constructs

The Nur77 construct was provided by Dr B. A. Osborne (University of Massachusetts, Amherst, MA). An expression vector for

GFP-fused mouse Nur77 (pEGFP-Nur77) was constructed by subcloning a PCR fragment of Nur77 into the pEGFP-C1 vector (Clontech). A Nur77-responsive luciferase reporter plasmid (NBRE-luc) (Katagiri *et al.* 1997) was provided by Drs Y. Katagiri and G. Guroff (National Institutes of Health, Bethesda, MD). Expression vectors for MAPKs (pSRαHA-ERK2 and pSRαHA-ERK5) and MAPKKs (pSRαHA-SASA for a dominant-negative form of MEK1, pSRαHA-ΔSESE for a constitutively active form of MEK1, pSRα-MEK5(A) for a dominant-negative form of MEK5, and pSRα-MEK5(D) for a constitutively active form of MEK5) were provided by Dr E. Nishida (Kyoto University, Kyoto, Japan). Dominant negative ERK5 (referred to here as dnERK5), where Thr219 and Tyr221 were replaced with Ala and Phe, respectively, was generated by a PCR-based method and subcloned into pcDNA3.1 (Invitrogen). A cDNA fragment of mouse ERK5 was subcloned into pcDNA3.1 in a reverse direction to knockdown endogenous ERK5.

In vitro kinase assay

Prior to the kinase assay for ERK5, DO11.10 cells were cultured in RPMI1640 containing 0.5% FCS for 4 h. After stimulation, cells were washed once with ice-cold PBS, and lysed in a lysis buffer solution (20 mM Tris–HCl, pH 7.5, 2 mM EGTA, 25 mM β-glycerophosphate, 1% Triton X-100, 2 mM dithiothreitol, 1 mM vanadate, 1 mM phenylmethylsulfonyl fluoride and 1% aprotinin), followed by centrifugation at 15 000 *g* for 30 min. The lysates were incubated for 2 h at 4 °C with an anti-ERK5 antibody along with protein A-Sepharose beads (Amersham Bioscience, Uppsala, Sweden). After washing 3 times with Tris-buffered saline containing 500 mM NaCl, the resulting immunoprecipitates were divided into two aliquots: one was used for the kinase assay, and the other for immunoblotting to evaluate the efficiency of immunoprecipitation. The immune complex was incubated at 30 °C for 30 min with a reaction buffer solution (20 mM Tris–Cl, pH 7.5, 10 mM MgCl$_2$ and 100 μM cold ATP along with 7.4 kBq of [γ-^{32}P]ATP) containing 10 μg of myelin basic protein (MBP) or GST-Nur77 as a substrate. In some experiment, GST-Nur77 was also incubated with the immunoprecipitates by an anti-ERK2 antibody. After SDS-PAGE, ^{32}P incorporated into the substrate was quantified on an image analyzer (BAS2000, Fujifilm, Tokyo, Japan).

DNA fragmentation assay

DNA fragmentation was detected as described previously (Hirt 1967). Briefly, DO11.10 cells (1 × 10^6) were incubated at room temperature for 1 h in a fragmentation buffer solution (10 mM Tris–HCl, pH 8.0, 10 mM EDTA and 0.6% SDS). NaCl was then added to a final concentration of 1 M and the samples incubated at 4 °C overnight. Nuclear debris was then spun down for 30 min at 15 000 *g* at 4 °C. The DNA fraction in the supernatant was prepared by QIAquick PCR purification kit (Qiagen), followed by incubation with 200 μg/mL RNase A at 37 °C for 2 h. Samples were then electrophoresed on a 1.5% agarose gel and visualized by ethidium bromide staining.

Annexin-V staining

After stimulation, DO11.10 cells were incubated with annexin-V-APC (BD Bioscience) in the presence of 1 mM CaCl$_2$ for 20 min at 4 °C, followed by washing with PBS containing 1 mM CaCl$_2$. Apoptotic cells were defined by APC-positive cells on a FACSCalibur.

Luciferase assay

To examine the transcriptional activation of Nur77, we employed luciferase assay system using NBRE-luc as a reporter (Katagiri *et al.* 1997). DO11.10 cells were transiently co-transfected with expression vectors for MAPKK and MAPK along with NBRE-luc in combination with pRL-TK (Promega, Madison, WI) for normalization by electroporation at 250 V, 960 μF. Luciferase activities in cell lysates were measured in triplicate on a luminometer (LB9507; Berthold, Bad Wildbad, Germany), using the Dual-Luc assay system (Promega).

References

Abe, J., Kusuhara, M., Ulevitch, R.J., Berk, B.C. & Lee, J.D. (1996) Big mitogen-activated protein kinase 1 (BMK1) is a redox-sensitive kinase. *J. Biol. Chem.* **271**, 16586–16590.

von Boehmer, H. (2004) Stimulation of the T-cell receptor: receptor-controlled checkpoints in T-cell development. *Adv. Immunol.* **84**, 201–238.

van den Brink, M.R., Kapeller, R., Pratt, J.C., Chang, J.H. & Burakoff, S.J. (1999) The extracellular signal-regulated kinase pathway is required for activation-induced cell death of T cells. *J. Biol. Chem.* **274**, 11178–11185.

Calnan, B.J., Szychowski, S., Chan, F.K., Cado, D. & Winoto, A. (1995) A role for the orphan steroid receptor Nur77 in apoptosis accompanying antigen-induced negative selection. *Immunity* **3**, 273–282.

Chen, C.-Y., Del Gatto-Konczak, F., Wu, Z. & Karin, M. (1998) Stabilization of interleukin-2 mRNA by the c-Jun NH2-terminal kinase pathway. *Science* **280**, 1945–1949.

Cobb, M.H. & Goldsmith, E.J. (1995) How MAP kinases are regulated. *J. Biol. Chem.* **270**, 14843–14846.